Isolating Advective Signatures in Temperature Logs

Von der Fakultät für Georessourcen und Materialtechnik
der Rheinisch-Westfälischen Technischen Hochschule Aachen

zur Erlangung des akademischen Grades eines

Doktors der Naturwissenschaften

genehmigte Dissertation

vorgelegt von **Dipl.-Ing.**

Andrei Zschocke

aus Berlin

Berichter: Univ.-Prof. Dr. rer. nat. Christoph Clauser
Univ.-Prof. Dr. rer. nat. Martin Sauter

Tag der mündlichen Prüfung: 29.06.2007

Abstract

Geothermics as a discipline of Geophysics deals with the description of the thermal regime, its variation in time, and the associated processes. These processes can be quantified by their characteristic thermal signature observed in temperature records. Heat transfer in the Earth's crust occurs primarily by thermal diffusion. On the other hand, heat advection due to groundwater flow in general is a more efficient transport mechanism. Therefore, the subsurface temperature field can be a sensitive indicator of even small flow rates. The challenge is to isolate the desired thermal signature from interfering signatures. This is achieved by eliminating the thermal signatures of all other processes and factors from the temperature data which may be caused by heterogeneity of thermal rock properties, heat generation, and transient variations of the ground surface temperature. Otherwise, these signatures may be misinterpreted leading to false conclusions.

This work focuses on quantifying groundwater flow (Darcy flow) and eliminating technical perturbations from temperature logs. Both main topics complement each other because the analysis of groundwater flow on temperature data will benefit from an improved database. In turn, the flow analysis provides useful information to constrain results from classic approaches, for instance interpretation of hydraulic data. The factors and processes which eventually disturb a flow analysis are introduced. The importance of disturbing effects depends on both magnitude and shape of the superposed thermal signatures.

Subsurface Darcy flow can be identified by its characteristic thermal signature. Here, a simple geothermal technique is proposed for quantifying regional strata-bound flow based on a detailed analysis of borehole temperatures. Depending on the spatial

data distribution and the involved heat transfer mechanisms this method yields results of different quality. In particular, the relation between subsurface flow and temperature gradient has a strong influence. In a case study with data from the Alpine Molasse Basin, the method yields a lower bound for the flow magnitude. Another case study is from the Dömitz-Lenzen area in northern Germany and yields the magnitude of the regional flow owing to a larger data set and information on the direction of flow from additional, independent information. Under optimum conditions, this method also yields an estimate of the direction of regional strata-bound groundwater flow as well as the uncertainty in magnitude and direction. Finally, the full potential of the method is demonstrated using a synthetic data set.

Ideally, a geothermal investigation is based on densely sampled, high-precision temperature logs from boreholes. They need to represent the formation temperature as accurately as possible. Often, temperature measurements influenced by the drilling process and the associated mud circulation are not of sufficient quality for geothermal methods. Horner's method is a widely used correction method which is based on an analysis of a time series of temperature records. Mostly, these data are not available and a correction is therefore not possible. The approach presented here in the second focus of this work enables to correct entire temperature logs even if no repeat measurements are available. This is achieved by combining the theory behind Horner's method with estimates of radial heat flow. Given a large number of technically perturbed logs, this new approach enlarges considerably the potential data base suitable for geothermal methods. The implications for two important fields of application are discussed: Analysis of fluid flow and of the ground surface temperature history.

Zusammenfassung

Geothermie ist eine Disziplin der Geophysik, die sich mit stationären oder transienten Einflüssen auf das Temperaturfeld im Untergrund beschäftigt. Die Temperaturverteilung kann charakteristisch ausgeprägt sein, so dass sich die einzelnen Prozesse anhand ihrer thermischen Signatur unterscheiden und quantifizieren lassen. Der dominierende Wärmetransportmechanismus in der Erdkruste ist die Diffusion. Weitaus effektiver breitet sich Wärme durch den Prozess der Advektion aus, so dass das Temperaturfeld im Untergrund ein sensibler Indikator für kleinste Grundwasserbewegungen sein kann. Darüber hinaus gibt es eine Reihe weiterer Einflüsse: Dazu zählen die Heterogenität der Gesteinseigenschaften, die Wärmeproduktion oder die paläoklimatische Veränderung der Temperatur an der Erdoberfläche. Die Herausforderung in der Interpretation von Temperaturdaten besteht im Wesentlichen darin, eine Signatur aus mehreren sich überlagernden Signaturen zu isolieren. Gelingt dies nicht vollständig, führt die Analyse, in Abhängigkeit von Signaturform und -amplitude, zu verfälschten Ergebnissen.

Ein Schwerpunkt dieser Arbeit ist die Quantifizierung des Grundwasserfließens (Darcy-Fließen) anhand der Analyse von Temperaturlogs. Im Vordergrund steht hier die neu entwickelte „Schichtfolgende Strömungsanalyse", mit der man Fluidbewegungen entlang von Horizonten bestimmen kann. Zudem wird auf Störeffekte eingegangen, die bei Strömungsanalysen beachtet werden müssen. Klassische Methoden, wie die Interpretation von hydraulischen Daten, stellen Fließregime im regionalen Maßstab oft ungenügend dar. Der vorgestellte Ansatz erweitert das Methodenrepertoire und bezieht in diesem Arbeitsumfeld weitgehend ungenutzte Daten mit ein. Man erhält, in Abhängigkeit von der räumlichen Datenverteilung und den stattfindenden Wärmetransportmechanismen, Ergebnisse unterschiedlicher Aussagekraft. Von entscheiden-

der Bedeutung ist dabei insbesondere das Verhältnis zwischen dem Grundwasserfluss und dem Temperaturgradienten. Eine Fallstudie aus dem Gebiet des Alpinen Molassebeckens ergab lediglich eine Untergrenze für den Betrag der Fließgeschwindigkeit. Bei einer weiteren Fallstudie aus dem Gebiet Dömitz-Lenzen im Norden Deutschlands konnte aus zusätzlichen, unabhängigen Daten zunächst die Richtung des Fließweges bestimmt werden. Durch diese Vorkenntnis war es möglich, den absoluten Betrag der Fließgeschwindigkeit abzuschätzen. Das gesamte Potenzial der Methode abzurufen, das heißt zusätzlich die Richtung regionalen Fließens zu bestimmen sowie Genauigkeit von Richtung und Betrag anzugeben, ist unter idealen Bedingungen, wie bislang nur in einem synthetischen Datensatz vorzufinden, möglich.

Neben den natürlichen Prozessen, die störend auf eine Strömungsanalyse wirken können, wird auf die Beseitigung technisch bedingter Störungen in den Temperaturdaten eingegangen. Dichte Temperaturlogs, welche die Formationstemperatur um die Bohrung so genau wie möglich widerspiegeln, sind die beste Voraussetzung für geothermische Untersuchungen. Durch Bohrbetrieb und Spülungsumlauf ist jedoch die erforderliche Qualität der Daten oft nicht gegeben. Das weit verbreitete „Horner-Verfahren", zur Korrektur dieser Effekte, kommt häufig nicht zum Zuge, da meist eine zeitliche Folge von Temperaturmessungen, auf denen das Verfahren basiert, nicht vorhanden ist. Es wird ein Ansatz vorgestellt, der es ermöglicht, Temperaturlogs zu korrigieren, selbst, wenn keine Wiederholungsmessungen vorliegen. Die Theorie des „Horner-Verfahrens" wird hierzu mit einer Abschätzung des radialen Wärmeflusses von der Bohrung in die Formation kombiniert. Im Hinblick auf die hohe Anzahl technisch gestörter Temperaturdaten, erweitert dieser Ansatz erheblich die potenzielle Datenbasis für geothermische Methoden. Die sich daraus ergebenden Implikationen werden für die Analyse von Fluidbewegungen diskutiert und für ein weiteres wichtiges Anwendungsfeld, „Die Rekonstruktion der Temperaturhistorie an der Erdoberfläche", beschrieben.

Preface

This work was carried out while I was employed at the Leibniz Institute for Applied Geosciences in Hannover. The studies mainly emerged from tasks I had been given within the project ”Geothermische Rasteranalyse”. The project was funded by the German Federal Environmental Ministry as part of the activities of its AkEnd Working Group (http://www.akend.de) through Office for Radiation Protection (BfS), contract No. 9X0009-8497-2 to Geophysica Beratungsgesellschaft mbH. Additionally, the BfS provided data from the hydrogeological and geothermal case study Dömitz-Lenzen. The Geological Surveys of Baden-Württemberg (LGRB, Freiburg) and Bavaria (GLA, München) made available core material and data from several geothermal boreholes in the study area. The Wirtschaftsverband Erdöl- und Erdgasgewinnung (WEG) kindly allowed the team to use material from their archives, which were supplied to us by the Erdölgeologischer Austausch (ATS) hosted at the Geological Survey of Lower Saxony (NLfB, Hannover).

I like to thank the colleagues Hilke Deetjen, Andreas Hartmann, Frank Höhne, Rüdiger Schellschmidt, Wolfram Rühaak and Reinhard Jung for their kind support. I am especially grateful to Volker Rath for numerous discussions from which I profited a great deal although he was at a remote place in Aachen - thanks to modern communication technology. I wish to thank my doctoral thesis supervisor Christoph Clauser for his support. His valuable suggestions and critical comments encouraged me and improved the quality of my work.

Ralf Gelfort, Hanna-Maria Rumpel and Slavica Babinka are warmly acknowledged for helpful comments on the manuscript. I am glad I could share recreative breaks with them.

The algorithms for Péclet number analysis and for correction of artificial transients in boreholes have been implemented into Matlab[1] code and are freely available either from me personally or downloaded from the website of the RWTH Aachen University (http://www.geophysik.rwth-aachen.de). Both main issues of this work which are mainly found in Chapter 3 and 4 are published in the "Journal of Geophysics and Engineering":

(1) Zschocke, A., Rath, V., Grissemann, C., and Clauser, C., Estimating Darcy flow velocities from correlated anomalies in temperature logs, J. Geophys. Eng., **2**, 332-342, 2005.

(2) Zschocke, A., Correction of non-equilibrated temperature logs and implications for geothermal investigations, J. Geophys. Eng., **2**, 364-371, 2005.

[1] Copyright 1984-2002, The MathWorks Inc.

The first time I got involved with geothermics was on a field trip to Goias in Central Brazil. Caldas Novas is the name of a little, rapidly grown town where half of the plots and buildings seem property of hotels offering thermal spas to their guests. Commercials inform that this area is the greatest thermal spring of the world. I asked myself whether they compare the energy flux or volume flux. But in the moment when I saw one of the major springs emerging form the edge of a table mountain I doubted no more that this is a very exceptional place. 1.4 $m^3 s^{-1}$ at 36 $°C$ is the impressive evidence of the enormous energy resource in the subsurface. Some wells had temperatures of even more than 60 $°C$. The basal heat flow in this area was on an average value. Locations such as Caldas Novas are often characterized by high permeability that provides hydraulic connection between deep, hot reservoirs and the spring. The temperature of the spring water reflects the efficiency of heat transfer by advection of groundwater. To understand geothermal systems in detail a combination of methods is necessary. The presented approaches in this work help to understand flow processes and improve the data base for geothermal methods. The common factor is expressed in the title ***Isolating Advective Signatures in Temperature Logs****.*

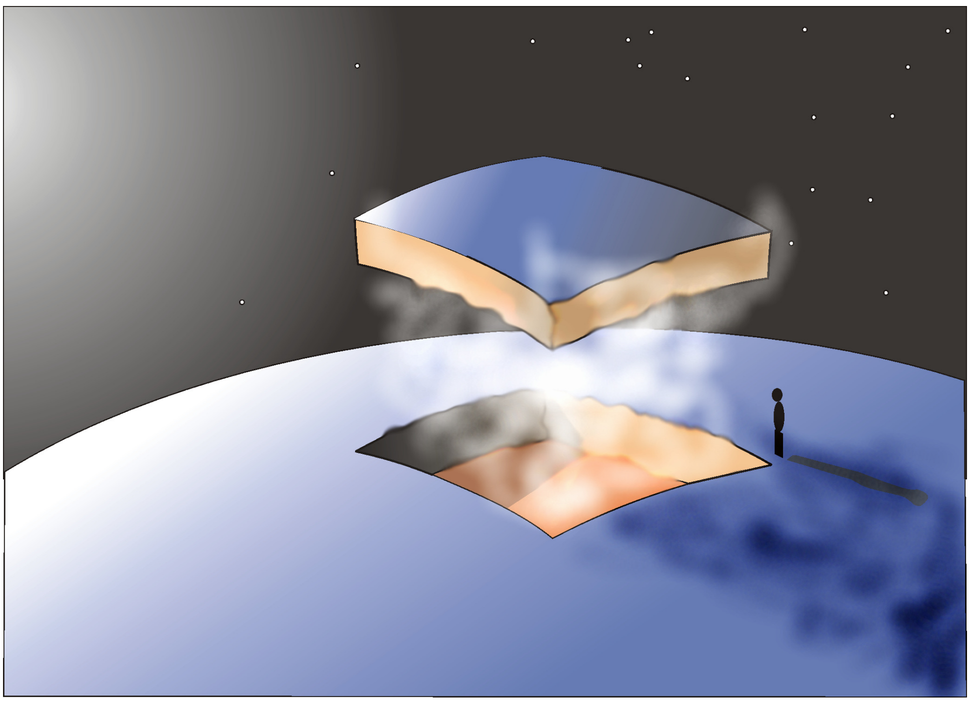

List of Symbols

Symbols	Definitions	Units
b	rate of boundary displacement	$m\,s^{-1}$
c	isobaric specific heat capacity	$J\,kg^{-1}\,K^{-1}$
H	heat generation rate	$W\,m^{-3}$
κ	thermal diffusivity	$m^2\,s^{-1}$
λ	thermal conductivity	$W\,m^{-1}\,K^{-1}$
Pe	Péclet number	1
q	specific heat flow	$W\,m^{-2}$
q_h	radial specific heat flow	$W\,m^{-1}$
r	radial distance to a borehole	m
ρ	density	$kg\,m^{-3}$
T	temperature	$^{\circ}C$
t	time	s
u	sedimentation/erosion rate	$m\,s^{-1}$
v	specific discharge (Darcy flow)	$m\,s^{-1}$
z	depth	m

Subscripts	
a	advective
b	fluid-matrix
c	mud circulation
D	dimensionless
eq	equilibrium
f	fluid
h	horizontal
m	drill mud
s	shut-in

Contents

List of Figures

Chapter 1

Introduction

1.1 Objective and outline

In general, temperature measurements in boreholes reveal an increase of temperature with depth. This is due to a constant heat flow from the Earth's interior to its surface where it is radiated into space. The total heat loss of the Earth amounts 4.42 10^{13} W (Pollack et al., 1993), whereas the heat generated by the decay of radiogenic isotopes is 2.75 10^{13} W (van Schmus, 1995). Thus, about 62 % of the energy required to maintain the global heat flow which averages averages 87 $\mathrm{mW\,m^{-2}}$ origins from radiogenic decay. Presently, only about 17 % of the energy originates from the heat released when the Earth was formed (Pollack et al., 1993).

Mostly, heat is transferred either by advection or by diffusion. Radiation becomes significant at temperatures above about 600 °C (Clauser, 1988). To understand the terrestrial temperature field, a number of factors have to be considered such as thermal conductivity, thermal diffusivity and heat generation of the rocks and pore fluids. In addition, heat flow from the mantle into the Earth's crust is unevenly distributed. Groundwater flow, paleoclimate and topographic evolution, i.e. uplift or subsidence of the crust coming along with erosion or sedimentation are processes that can be also important. Amongst those, groundwater flow or advective transport in general is the most efficient heat transfer mechanism. Therefore, the subsurface temperature field is a sensitive indicator even of small specific discharge on the order of few mm per year.

In consequence, geothermal methods have the potential to quantify the above mentioned processes by interpretation of its characteristic thermal signature in the subsurface. This requires, however, the prior assessment and elimination from the data of all other processes contributing to the temperature field. Otherwise, unaccounted influences with similar signatures could be misinterpreted and lead to wrong results. In a simple scenario assuming heat transfer only by diffusion and a constant vertical basal heat flow, a temperature log would be piecewise linear. Temperature logs of a curved shape indicate groundwater flow, transient diffusion or can be caused by 3D effects in steady-state heat conduction. For instance, Péclet number analysis yields the vertical discharge rate from an analysis of curved temperature profiles (Bredehoeft and Papadopulos, 1965; Clauser, 1999).

Other classic approaches for detecting and quantifying regional groundwater flow are challenging and have certain disadvantages. Studies of artificial and natural tracers require a long observation time. Indirect methods like well tests estimate pressure and hydraulic permeability but can infer fluid velocities only by assuming plausible driving forces. Inhomogeneity of the underground is a source of error in the interpretation of well tests: If a single fracture contributes most of the flow, results from piezometric measurements do not represent an average value on a large scale. In contrast to temperature measured in boreholes, advective temperature signals propagate into the host rock by thermal diffusion and can be observed at a large distance, depending on the travel time.

The magnitude of heat transfer by advection of fluids depends on the discharge rate and the angle subtended between the flow vector and the direction of temperature gradient. A flow vector which is directed parallel to the isotherms causes no net heat transfer. Therefore, geothermal methods have an important restriction in common: They detect only the flow component in the direction of temperature gradient. As the geothermal gradient is predominantly vertical, flow analysis on temperature data is most sensitive to vertical groundwater flow.

Groundwater flow along thin, nearly horizontal aquifers may contribute an important amount of flow in sedimentary basins. The corresponding lateral heat advection may be sufficiently strong to create characteristic thermal signatures from which the flow can be estimated (van der Kamp and Bachu, 1989; Vasseur and Demongodin, 1995). Measurements revealed that vertical heat flow above the aquifer changes proportional to the heat advected within a confined layer (Ziagos and Blackwell, 1981). This motivated development of a method for quantifying Darcy velocity along layers based on the change of vertical heat flow across reservoirs.

This method requires estimating the temperature distribution in the aquifer. Therefore, at least three temperature logs are needed. Heat flow logs are derived from these temperature logs and profiles of thermal rock conductivity. Because of the restriction in geothermal methods explained above, in such a scenario only a minimum estimate of the Darcy flow is obtained (case a). The magnitude of the flow can be derived if the flow direction is known, as each anomaly results from projecting the vector of heat advection projected onto the thermal gradient vector (case b). Usually the flow direction is unknown. But in case that the nonlinear temperature field within the layer is available and heat flow logs from different boreholes show the corresponding anomaly, the method yields estimates of the flow direction, its magnitude, and corresponding errors (case c). This case requires more than three temperature logs to derive the temperature field.

In the Alpine Molasse basin the analysis of three deep temperature logs revealed an anomalously high vertical heat flow above a known regional aquifer. The available data set allowed to estimate the Darcy flow according to case (a) (Chapter 3.2). In the case study of heat flow logs in the Dömitz-Lenzen area in Germany (Chapter 3.3) the flow direction is known from an associated anomaly in groundwater salinity which was traced by measurements in many boreholes. The analysis of heat flow logs from those boreholes yielded the magnitude of flow. This study corresponds to case (b). Up to now an ideal data set to show case (c) was missing. Therefore, the full potential of the method is demonstrated on synthetic data from a numerical simulation. The analysis of this data is shown in Chapter (3.4).

Beside natural processes and factors which are superposed on the advective signal, thermal data frequently contain signatures of technical perturbations associated with drilling and circulating mud. These create a transient perturbation of the temperature field around the borehole (Bullard, 1947).

To obtain equilibrated formation temperatures it is necessary to wait until this perturbation has dissipated. Because of the associated long shut-in times of several weeks or months this is often not possible in commercial boreholes. However, perturbed temperature logs do not always need to be excluded from a geothermal analysis as they still contain useful information on the temperature field. Much research has been concerned with reconstructing the undisturbed formation temperature from perturbed data (e.g. Horner, 1951; Lachenbruch and Brewer, 1959; Dowdle and Cobb, 1975; Vasseur et al., 1985; Kutasov, 1999). The novel technique presented here was developed to correct technically induced thermal transients that up to now could not be corrected by the existing methods. It has the potential to expand considerably the available data base for geothermal investigations.

Beyond the novel techniques introduced above, this thesis discusses factors and processes that might disturb a flow analysis on temperature data. Following this first introductory chapter, Chapter (2) introduces the basic theoretical background of heat transfer in the subsurface and treats factors that might distort a temperature log. In Chapter (3) a method is presented for quantifying Darcy flow along inclined aquifers from an analysis of heat flow anomalies in logs. Chapter (4) addresses the perturbation induced by drilling and mud circulation in temperature logs. Finally, implications for different geothermal studies are analyzed. In the Discussion (Chapter 5), sources of error and possible fields of application are treated. In the Conclusion (Chapter 6), the potential and the significance of the methods proposed in this study are pointed out.

1.2 Temperature data

Any geothermal analysis requires accurate information on the thermal regime. The bulk of temperature measurements consists of temperature logs. Densely sampled, high-precision temperature logs are optimum data because the magnitude of an expected temperature signature of a certain process or factor may be less than one Kelvin. The petroleum industry has drilled most of the boreholes. The data distribution reflects the industry's activities associated with oil and gas exploration. Therefore, lateral resolution of temperature data is often unsatisfactory whereas vertical sampling rate is dense.

Often, spatial interpolation of anisotropic and scattered data is challenging and needs to be constrained by independent information on the geological structure and the governing processes. For this study, the data base of the *Leibniz Institute for Applied Geosciences* formed the base of a Germany-wide temperature mapping (Fig. 1.1). A considerable part of the data are Bottom Hole Temperatures (BHT) that were corrected by Horner's method, but still contain an error margin of $\pm$ 5 K, on average [1]. The data was first interpolated onto a horizon in the vertical and then interpolated laterally.

The highest temperature anomalies are observed in the Rhein graben in southwestern Germany. This region is known for its high potential for geothermal energy. Beside the increased basal heat flow of up to 140 $\mathrm{mWm^{-2}}$ locally, the magnitude of anomalies suggest associated groundwater flow because they cannot be explained by thermal diffusion only. The trends and patterns in the temperature map (Schellschmidt and Zschocke, 2003) for a depth of $1000\,\mathrm{m}$ b.g.l. (Fig. 1.1) are certainly biased by the quality of the data and its uneven distribution. However, the variability of the temperature field is clearly due to the numerous factors and processes affecting the thermal regime.

[1] Schellschmidt R. (GGA-Institut), personal communication, 2004.

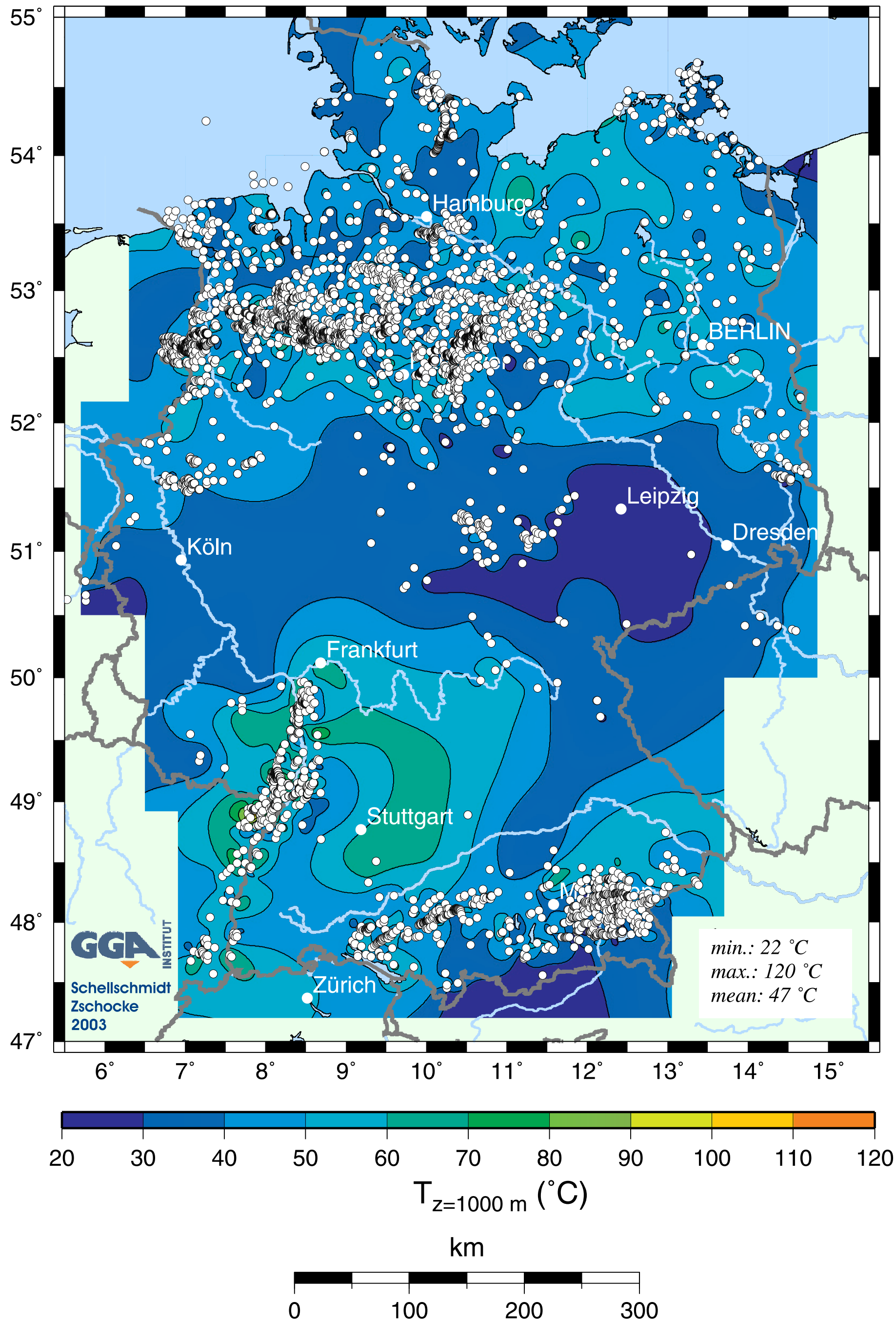

Fig. 1.1: Example of a temperature map of Germany (Schellschmidt and Zschocke, 2003) showing borehole locations and temperature at a depth of 1000 m b.g.l.. The variable temperature distribution in the Earth's crust is the result of several processes which superpose each other.

1.3 Potential fields of application

Analysis of temperature data provides critical input to a number of scientific and technical questions, both in exploration and engineering. This section addresses two currently discussed fields of application which may profit from of the high potential of geothermal methods for identifying and quantifying fluid flow.

In many countries the selection of appropriate sites for the **deposition of hazardous material** in the deep subsurface is a ongoing and much debated issue. Potential repository sites need to satisfy a number of requirements. One crucial criterion requires a vanishing or no flow to prevent transport of poisonous or radiogenic substance to the biosphere. Therefore, thermal methods were developed to detect and quantify minute flow rates in the deep subsurface (Clauser et al., 2004). It was demonstrated that geothermal methods often provide the best available approach for characterizing flow regimes in the deep subsurface.

The increasing world energy demand and the need to avoid CO_2-emissions make **renewable energy sources** an attractive option. Geothermal energy occupies a special position amongst renewable energy sources due to its continuous availability. It can therefore be used to provide base load energy for both thermal and electrical supply. Modern conversion techniques enable electrical power to be generated at temperatures from 100 $°C$. However, this technique becomes economically viable at temperatures above 150 $°C$ (Clauser, 2006). Thus, geothermal heat production is interesting even in regions with a modest temperature gradient of 25 $K\ km^{-1}$. Hot aquifers, crystalline rocks, and faults zones are important exploitable reservoir types (Paschen et al., 2003). To minimize economical risks, potential investors demand a prediction of the technical and geological risks. In the future, detailed temperature mapping and classification of areas with respect to thermal and hydraulic rock properties will be required for this purpose. In this context, a high temperature gradient, high rock permeability and groundwater flow rates are favorable. In general, these criteria are inverse to the ones used for characterizing good repository sites. Thus, thermal methods which are used in both cases are suitable for both applications.

Chapter 2

Influences on subsurface temperatures

2.1 Heat transfer mechanisms

Regions with higher molecular kinetic energy pass their thermal energy to regions with less molecular energy through direct molecular collisions, a process known as heat conduction or **thermal diffusion**. However, when heat is transferred into fluids in motion, most often the dominant transport process will be **advection** (forced convection). This requires a hydraulic gradient to drive the fluid motion which may be generated, for instance, by topography, unevenly distributed groundwater recharge, density contrast in the fluid, or transient porosity. When a fluid is heated its volume expands. As a result of the correspondingly reduced density the fluid parcel becomes buoyant and rises. Such heat-induced fluid motion in initially static fluids is known as free convection. Density induced fluid motion may also be caused by different concentrations of dissolved solids such as in brines.

2.1.1 Thermal diffusion

Thermal diffusion requires a temperature gradient. Thus, it is ubiquitous in the Earth's crust. **Fourier's law** applies for steady-state heat conduction without heat generation and is defined for anisotropic media as:

$$\begin{pmatrix} q_x \\ q_y \\ q_z \end{pmatrix} = - \begin{pmatrix} \lambda_{xx} & \lambda_{xy} & \lambda_{xz} \\ \lambda_{yx} & \lambda_{yy} & \lambda_{yz} \\ \lambda_{zx} & \lambda_{zy} & \lambda_{zz} \end{pmatrix} \cdot \begin{pmatrix} \frac{\partial T}{\partial x} \\ \frac{\partial T}{\partial y} \\ \frac{\partial T}{\partial z} \end{pmatrix} \tag{2.1}$$

or written in a more simple way

$$\overrightarrow{q} = -\underline{\lambda}\,\nabla T\ . \tag{2.2}$$

This equation defines the specific heat flow q ($\mathrm{W\,m^{-2}}$) for a given temperature distribution T ($^{\circ}\mathrm{C}$) and thermal conductivity λ ($\mathrm{W\,K^{-1}m^{-1}}$). x, y, z indicate the direction of the cartesian coordinates with z being positive downward. Geothermal problems are often reduced to one dimension because the direction of maximum heat flow is approximately vertical. In particular, when only the vertical component of the temperature gradient can be computed from temperature logs thermal conductivity is reduced to its z-component and treated as scalar:

$$q \doteq q_z = -\lambda_{zz}\,\frac{\partial T}{\partial z} = -\lambda\,\frac{\partial T}{\partial z}. \tag{2.3}$$

In the steady state, the difference between the heat flowing into and out of a control volume equals the heat generation rate H ($W\ m^{-3}$) within the volume:

$$\nabla \cdot \overrightarrow{q} = H. \tag{2.4}$$

Substituting $\overrightarrow{q}$ from Fourier's law (Eq. 2.2), one arrives at the generalized diffusion equation:

$$\nabla \cdot (\lambda\,\nabla T) + H = 0. \tag{2.5}$$

Transient processes are described by the amount of heat stored in a control volume over time:

$$\nabla \cdot (\lambda\,\nabla T) + H = (\rho\,c)_b \frac{\partial T}{\partial t}\ . \tag{2.6}$$

Here, ρ is density ($\mathrm{kg\,m^{-3}}$), c isobaric specific heat capacity ($\mathrm{J\,kg^{-1}K^{-1}}$) and the subscript b refers to bulk properties. Assuming thermal conductivity to be constant and isotropic it can be taken out of the differentiation. One finally obtains

$$\frac{\lambda}{(\rho c)_b}\,\nabla^2 T + \frac{H}{(\rho\, c)_b} = \frac{\partial T}{\partial t}, \tag{2.7}$$

where $\lambda/(\rho\, c)_b$ is the thermal diffusivity κ. In the most simple case we assume purely conductive steady-state conditions and a negligible effect of heat generation as is often the case in sediments. Regarding only the z-component Eq. 2.7 reduces to:

$$0 = \lambda \frac{\partial^2 T}{\partial z^2}\,. \tag{2.8}$$

The solution of this equation yields a linear temperature increase with depth. Temperature can then be calculated at any depth from surface specific heat flow q_0 and the ground surface temperature $T(z_0)$ with z being positive downward by:

$$T(z) = T(z_0) + \frac{q_0}{\lambda_b} z\,. \tag{2.9}$$

2.1.2 Advection of fluid

Heat advection occurs when fluid temperature changes along the flow path. The specific discharge rate $\overrightarrow{v}$ ($\mathrm{m\,s^{-1}}$) in a porous medium is defined by Darcy's law (Darcy, 1856) as

$$\overrightarrow{v} = \frac{k \rho_f g}{\mu}\,\nabla h, \tag{2.10}$$

where k is permeability ($\mathrm{m^2}$), g gravity ($\mathrm{m\,s^{-2}}$), μ dynamic viscosity ($\mathrm{Pa\,s}$), and h hydraulic head (m). Heat transport in an isotropic porous medium (λ_b constant) including heat advection is described by:

$$\frac{\partial}{\partial t}\left[(\rho\, c)_b T\right] = \underbrace{\nabla \cdot \lambda_b\, \nabla T}_{conduction} - \underbrace{(\rho\, c)_f\, \overrightarrow{v} \cdot \nabla T}_{advection} + H, \tag{2.11}$$

where the subscript f refers to fluid properties.

Vertical heat advection introduces curvature in a temperature log (Fig. 2.1, left panel). In a vertical Péclet number analysis, the vertical Darcy flow rate is determined from an interpretation of this characteristic thermal signature (Bredehoeft and Papadopulos, 1965; Mansure and Reiter, 1979; Sass and Lachenbruch, 1982; Clauser and Villinger, 1990). The remarkable sensitivity of this method is due to the fact that here the flow is directed parallel to the temperature gradient. In its most simple form, the analysis requires only one temperature log which is an important advantage in view of the often scattered data available.

Assuming constant vertical specific discharge and constant thermal conductivity the one-dimensional steady-state heat transport equation is:

$$0 = \lambda_b \, \frac{\partial^2 T}{\partial z^2} - (\rho\, c)_f \; v_z \, \frac{\partial T}{\partial z} \tag{2.12}$$

(Stallman, 1963; Bredehoeft and Papadopulos, 1965). Rearranging gives

$$\frac{\partial^2 T}{\partial z^2} = \frac{(\rho\, c)_f}{\lambda_b} \; v_z \, \frac{\partial T}{\partial z} \; . \tag{2.13}$$

The Péclet number (Pe) is defined as the ratio of advective (subscript a) and conductive (subscript c) heat transfer:

$$Pe = \frac{q_a}{q_c} = \frac{(\rho\, c)_f \, v \, \Delta T}{\lambda_b \left(\frac{\Delta T}{L}\right)} = \frac{(\rho\, c)_f \, v \, L}{\lambda_b} \; . \tag{2.14}$$

Accordingly, Pe/L is given by

$$\frac{Pe}{L} = \frac{(\rho\, c)_f \, v}{\lambda_b} \; , \tag{2.15}$$

where L is the distance over which the fluid flows. Inserting Pe/L in Eq. 2.13 and v being equal to v_z one obtains

$$\frac{\partial^2 T}{\partial z^2} = \frac{Pe}{L} \, \frac{\partial T}{\partial z} \tag{2.16}$$

(Mansure and Reiter, 1979). Knowing Fourier's law $q = -\lambda \frac{\partial T}{\partial z}$ one can account for changing thermal conductivity for instance in a stratified subsurface by multiplying Eq. 2.16 by the thermal conductivity $\lambda(z)$ yielding:

$$\frac{\partial q(z)}{\partial z} = \frac{Pe}{L} \; q(z) \; . \tag{2.17}$$

Integration yields

$$q(z) = q_0 \, e^{z \, \frac{Pe}{L}} \, . \tag{2.18}$$

Sass and Lachenbruch (1982) provided this solution which allows to asses Pe/L by evaluating the slope of a linear trend to the corresponding vertical heat flow profile on a logarithmic scale (Fig. 2.1, right plate). In a simple scenario with uniform thermal parameters the vertical component of Darcy flow is given by solving Eq. 2.15 for v:

$$v = \frac{Pe}{L} \cdot \frac{\lambda_b}{(\rho \, c)_f} . \tag{2.19}$$

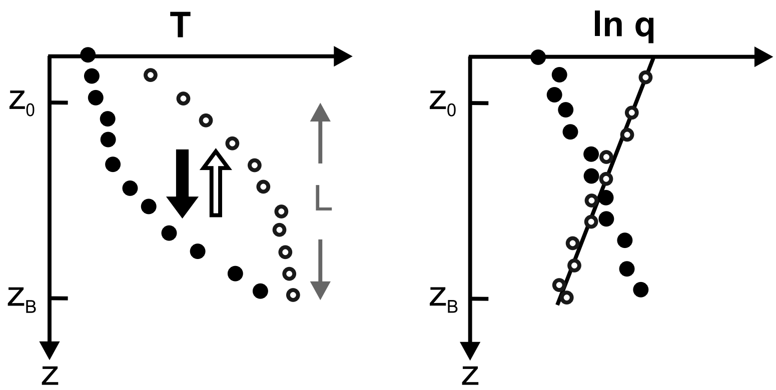

Fig. 2.1: Left panel: Upward and downward flow induces concave and convex curvature, respectively, in a temperature log. L equal to $\mathrm{z_B - z_0}$ is the distance over which the fluid flows. Right panel: The Péclet number is obtained by fitting a linear trend to the corresponding vertical heat flow profile on a logarithmic scale. The slope of the trend equals the Péclet number divided by the depth interval, $\mathrm{Pe/(z_B - z_0)}$.

Bredehoeft and Papadopulos (1965) provided an analytical solution for the one-dimensional Eq. 2.16:

$$T(z) = T_0 + \frac{q_0 L}{\lambda_b} \cdot \frac{e^{-z \frac{P_e}{L}} - 1}{e^{-P_e} - 1} \, . \tag{2.20}$$

They assumed one layer of constant thermal conductivity and a vertical groundwater flow over a depth interval $L \, (m)$, between z_0 and z. In this equation T_0 ($°C$) and q_0 are temperature and vertical specific heat flow at $z = z_0$, respectively.

To demonstrate the impact of flow on temperatures logs several hypothetical scenarios are calculated according to Eq. (2.20) with the parameters listed in Tab. (2.1) and the resulting temperature logs shown in Fig. (2.2). The larger the flow rate, the greater is the curvature. Upward and downward flow results in concave and convex temperature logs, respectively. Eq. 2.20 implies that the distance L over which the flow occurs is equally important for the magnitude of the thermal impact. Even flow rates on the order of a centimeter per year may induce anomalies of several Kelvin (ΔT_{flow} in Tab. 2.1) if the flow occurs over a large depth interval (in this case L = 1000 m).

Tab. 2.1: Parameter list for synthetic logs assuming vertical flow scenarios. The resulting temperature logs are depicted in Fig. (2.2). ΔT_{flow} is the amplitude of the thermal anomaly due to the fluid flow with respect to a purely conductive regime.

	Scenario						
Parameters	I	II	III	IV	V	VI	VII
$P_e\,(1)$	-3	-2	-1	$\rightarrow 0$	1	2	3
$\lambda\,(W\,m^{-1}K^{-1})$	2.5	2.5	2.5	2.5	2.5	2.5	2.5
$q_0\,(W\,m^{-2})$	-0.092	-0.187	-0.35	-0.6	-0.95	-1.39	-1.9
$L\,(m)$	1000	1000	1000	1000	1000	1000	1000
$\frac{q_0}{\lambda}/\frac{P_e}{L}\,(K)$	10	30	130	$\rightarrow \infty$	-350	-260	-230
$v_f\,(m\,a^{-1})$	-0.079	-0.053	-0.026	$\rightarrow 0$	0.026	0.053	0.079
$\Delta T_{flow}\,(K)$	8.2	5.7	3	0	3	5.7	8.1

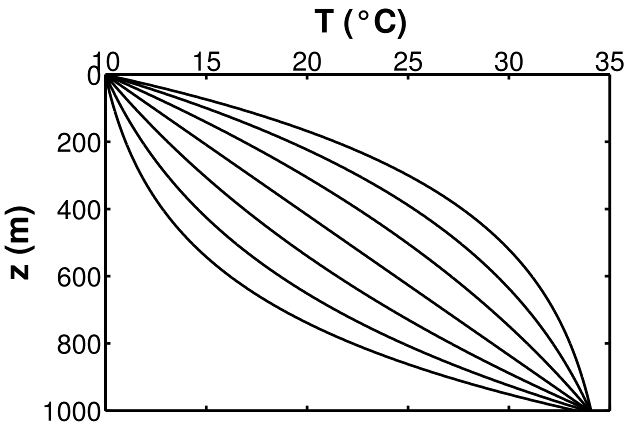

Fig. 2.2: Synthetic temperature logs calculated according to Eq. (2.20) for scenarios I - VII, from left to right. Assumed are different Darcy flows between $-0.08\ \mathrm{m\,a^{-1}}$ and $0.08\ \mathrm{m\,a^{-1}}$. The set of parameters is listed in Tab. (2.1). The higher the flow rate, the greater the curvature.

The derivative $\partial T(z)/\partial v(z)$ allows to identify log intervals of high sensitivity to the flow processes. This is important for a discussion of ambiguous thermal signatures in temperature logs induced by different processes. According to the chain rule, the derivative is given by the product of the corresponding derivatives of Eq. (2.20) and Eq. (2.15):

$$\frac{\partial T}{\partial v} = \frac{\partial T}{\partial Pe} \cdot \frac{\partial Pe}{\partial v} \quad . \tag{2.21}$$

The solution is

$$\frac{\partial T}{\partial v}(z) = \underbrace{\frac{q_0\, L}{\lambda}\left(-\frac{z}{L}\cdot\frac{e^{-z\cdot\frac{Pe}{L}}}{e^{Pe}-1} + \frac{e^{Pe}\cdot e^{-z\cdot\frac{Pe}{L}}-1}{(e^{Pe}-1)^2}\right)}_{\partial T/\partial Pe} \cdot \underbrace{\frac{(\rho c)_f\, L}{\lambda_b}}_{\partial Pe/\partial v} \quad . \tag{2.22}$$

Consider, for example, a downward groundwater flow of magnitude 0.02, 0.15 and $0.4\ \mathrm{m\,a^{-1}}$. Synthetic temperature logs (Fig. 2.3) can be derived using Eq. (2.20) and the corresponding derivatives from Eq. (2.22) (Parameters: T_0 =10 °C; $q_0 = 65\ \mathrm{mW\,m^{-2}}$; $\lambda_b = 2.5\ \mathrm{W\,m^{-1}\,K^{-1}}$; $L = 1000\ \mathrm{m}$; $z_0 = 0\ \mathrm{m}$; and $(\rho c)_\mathrm{f} = 2.3 \cdot 10^6 \mathrm{J\,m^{-3}\,K^{-1}}$).

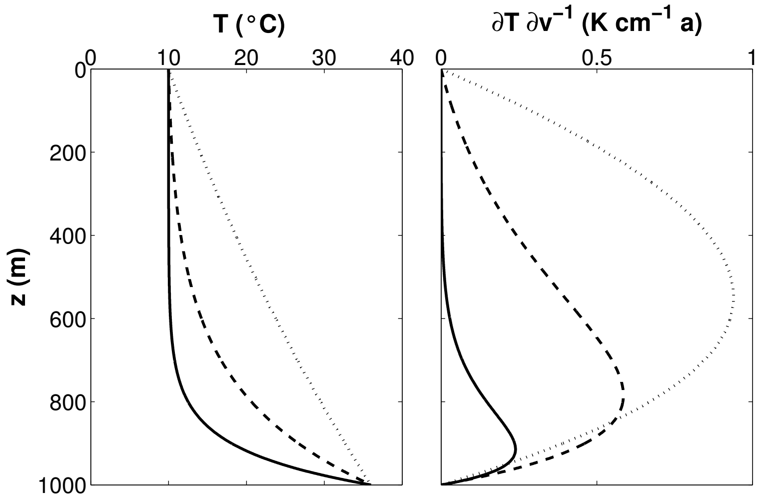

Fig. 2.3: Left panel: Synthetic temperature logs according to Eq. 2.20. Assumed are different Darcy flows: 0.02, 0.15 and $0.4\ \mathrm{m\,a^{-1}}$ (dotted, dashed and solid curve, respectively). Right panel: The corresponding derivatives according to Eq. (2.22) show the sensitivity of the temperature to the Darcy flow.

The derivatives (Fig. 2.3, right panel) show that the temperature profile in the case with a the highest flow rate of $0.4\ \mathrm{m\,a^{-1}}$ (solid curve) is less sensitive to changes in the discharge rate. Furthermore one can see that with higher flow rate the sensitive portion of the temperature log moves to the bottom. If L is much larger than the length disturbing signature, both signatures can easily be distinguished and isolated.

2.2 Heterogeneity and anisotropy of rock properties

Thermal conductivity of rocks quantity depends on the relative proportions of its mineral constituents and their geometrical relationship. Porosity is very important because pore fluids, such as water, brine, oil, and partially air or gas have low thermal conductivity compared to most minerals. Methods for estimation of thermal conductivity from the mineral content are based on averaging using harmonic, arithmetic, geometric, or square-root means. The algorithm chosen must suit both the structure of the subsurface and the texture of the rocks. For a horizontally layered subsurface, the harmonic mean is the model that fits best.

Eq. 2.9 implies a piecewise linear temperature profile if each lithological unit has a homogeneous thermal conductivity. In other words, the thermal gradient is constant within a layer and heat flow is constant over the entire profile. This model may fail if compaction of sediments decreases porosity with depth which would be accompanied by a progressive increase of thermal conductivity. In such a case, compaction models using an exponential, reciprocal or power law model are useful to interpolate thermal conductivity.

Dipping layers over large depth intervals experience increasing temperatures with depth. Then, an analysis of data needs to account for the decrease of thermal conductivity with temperature. Non-horizontal layering or laterally varying thermal conductivity refract the flow of heat away from the vertical. Salt domes have comparatively high thermal conductivity - more than twice the mean conductivity of other sediments (Beardsmore and Cull, 2001). Due to diapirism they form vertical structures focussing heat flow in the diapir. Consequently, a decrease of regional heat flow is observed adjacent to the diapir. A one-dimensional analysis would not be appropriate here. Elevated heat flow above a diapir may also be due to the transient effects of uplift and erosion.

Thermal conductivity can be measured in the laboratory on cores, crushed samples, or well cuttings. Commonly used devices are divided bar, needle probe, or thermal conductivity scanning (TCS) (Popov et al., 1999). Geophysical log parameters sensitive to porosity, such as resistivity, neutron absorption, gamma ray, sonic velocity, or density, can be used to estimate thermal rock conductivity along a borehole (Hartmann et al., 2005).

2.3 Heat generation

Heat generated by the decay of radioactive elements is a major internal heat source of the Earth. The important decay series are uranium (U), thorium (Th) and potassium (K). The isotopes $^{238}\mathrm{U}$ and $^{232}\mathrm{Th}$ are the primary heat producers today and are mainly found in crystalline rocks. $^{40}\mathrm{K}$ and $^{235}\mathrm{U}$ were more important in the Earth's early history. In sediments, the heat generation is often less significant and therefore neglected. Surface heat flow is related to the heat generation of the underlying basement rocks. In one dimension (z), the steady-state heat conduction equation is

$$0 = \lambda \, \frac{\partial^2 T}{\partial z^2} + H. \tag{2.23}$$

Integrating twice with respect to z and observing that $q(z=0) = q_0$ and $T(z=0) = T_0$ this yields:

$$T(z) = T_0 + \frac{q_0}{\lambda} \, z - \frac{H}{2\,\lambda} \, z^2. \tag{2.24}$$

The quadratic term indicates that non vanishing heat generation is a source of non-linearity in vertical temperature profiles. Thus, this process introduces curvature in temperature logs such as heat advection does. For logs through heat producing formations, the heat production needs to be assessed and the corresponding thermal signature - the term $H\,z^2/2\lambda$ in Eq. (2.24) - removed from the data before advective signatures are identified and interpreted.

2.4 Ground surface temperature history

Temperature signals from past climates can still be detected in today's subsurface temperature field. They diffuse from the ground surface into the subsurface and distort linear temperature gradients. The amplitude of this signature and the depth at which it is found depend on magnitude and frequency of the temperature variation at the Earth's surface. Seasonal changes propagate into the ground to depths of several meters whereas in Central Europe the amplitude of the signal of the last ice age (Fig. 2.4), 10^4 a ago, is preserved at depths between 1200 m and 1500 m (Clauser et al., 1997). From an inversion of temperature logs the ground surface temperature (GST) history can be inferred utilizing inversion techniques (e.g. Shen and Beck, 1991, 1992; Beck et al., 1992; Mareschal and Beltrami, 1992). This is of increasing interest since borehole temperature is a valuable proxy for the paleoclimate. Advective transport may be masked by this transient signature (Taniguchi et al., 1999a,b). The implications for a groundwater flow analysis on thus disturbed data are discussed in Chapter (4.4.2).

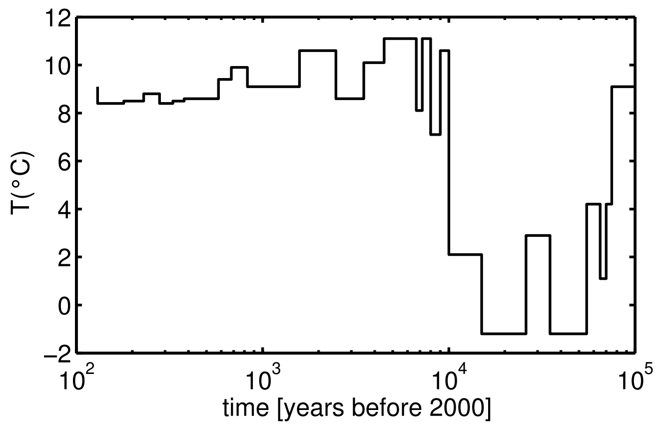

Fig. 2.4: Variations of the Earth's surface temperature in Central Europe after Haenel et al. (1988). The largest step at 10 000 a is the signature of the last ice age.

2.5 Topographic evolution

Vertical displacement of the Earth's surface driven by tectonic forces and fluid flow are both processes which transport heat by advection and induce curvature into temperature logs (e.g. Kohl. et al., 2001). For sedimentary basins and orogenic zones vertical rates of displacement may amount to several millimeters per year. Isostatic compensation of the load of ice shields is another driving force. The topographic evolution is accompanied by either sedimentation or erosion. Thus, the vertical displacement may be compensated by erosion or sedimentation, so that the position of the ground surface remains constant. The differential equation describing heat advection by a one-dimensional moving boundary is

$$\frac{\partial T}{\partial t} + u\frac{\partial T}{\partial z} = \kappa\frac{\partial^2 T}{\partial z^2}\,. \tag{2.25}$$

The depth z is positive downwards, u is the rate of the vertical displacement with respect to a point fixed on the moving boundary. Positive u corresponds to sedimentation, and negative u to erosion. The corresponding solution is

$$\begin{aligned} T(z,t) &= T_0 + \Gamma(z-u\,t) + \frac{1}{2}\left[\Gamma + \frac{\Gamma^* b}{u}\right] \\ &\cdot \left[(z+u\,t)\,e^{\left(\frac{u\,z}{\kappa}\right)}\;\; erfc\left(\frac{z+u\,t}{2\sqrt{\kappa\,t}}\right)\right. \\ &- \left.(z-u\,t)\;\; erfc\left(\frac{z-u\,t}{2\sqrt{\kappa\,t}}\right)\right], \end{aligned} \tag{2.26}$$

where b is the rate of displacement of the boundary with respect to a fixed reference, $\Gamma = \partial T/\partial z$ the initial, undisturbed temperature gradient at $\mathrm{t} = 0$, $\Gamma^* = \partial T_0/\partial z$ the vertical gradient of the Earth's surface temperature with elevation, and T_0 surface temperature at $\mathrm{z} = 0$ (Carslaw and Jaeger, 1959, p. 388).

I calculated hypothetic scenarios according to Eq. (2.26) assuming an isotropic and homogeneous thermal conductivity of 3 $\mathrm{W\,m^{-1}\,K^{-1}}$ and a thermal diffusivity of $10^{-6}\ \mathrm{m^2\,s^{-1}}$ over a period of 5000 years. The vertical tectonical displacement b (in $\mathrm{mm\,a^{-1}}$) was set to -6, -4, -2, 0, 1, 2, and 3. In this scenario (Fig. 2.5, left panel) the displacement of the medium is completely compensated by sedimentation or erosion rate u ($b + u = 0$). Another scenario has the same erosion rate u (6, 4, 2, 0, -1, -2, and 3, in $\mathrm{mm\,a^{-1}}$) and a constant uplift rate of of 1 $\mathrm{mm\,a^{-1}}$ (Fig. 2.5, right panel).

This process induces thermal signatures similar to those induced by fluid flow. Temperature logs from sedimentary basins with a rate of subsidence on the order of several $\mathrm{mm\ a^{-1}}$ will show signatures of comparable magnitude as those produced by steady-state heat advection. In such a case, the effect needs to be assessed and the corresponding signatures eliminated from the temperature data prior to any thermal flow analysis.

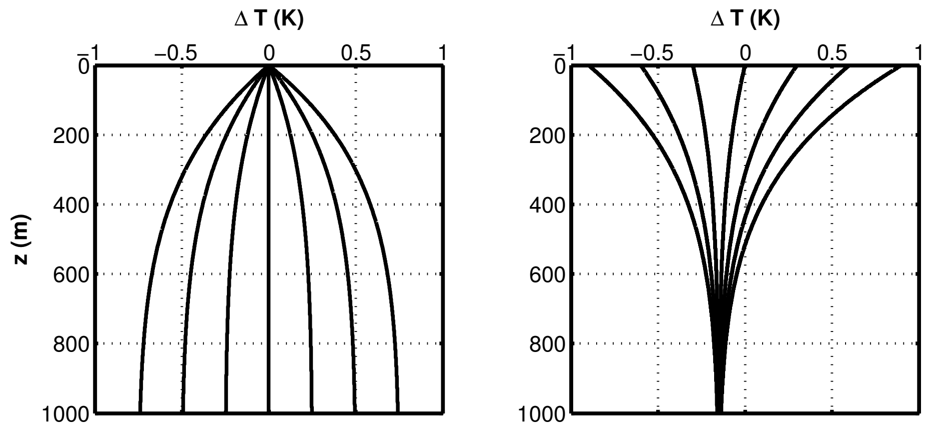

Fig. 2.5: Temperature signature $\Delta T = T(z, t = 5000) - T(z, t = 0)$ due to a vertical tectonic displacement associated with sedimentation and erosion after 5000 years. Left panel: tectonical displacement b in $\mathrm{mm\,a^{-1}}$ equals -6, -4, -2, 0, 1, 2, and 3, from left to right. In this scenario the displacement of the medium is completely compensated by sedimentation or erosion ($b + u = 0$). Right panel: same scenario except a constant rate of tectonical displacement b of 1 $\mathrm{mm\,a^{-1}}$ is assumed.

Chapter 3

Estimating strata-bound Darcy flow

Vertical Péclet analyses (Chapter 2.1.2) of advective signatures in temperature logs yield only the vertical component of flow. But in many sedimentary basins horizontal or strata-bound flow prevails. Advective heat transfer in these confined structures is often sufficiently strong to create characteristic signatures which can be observed in a closely sampled temperature log (van der Kamp and Bachu, 1989; Reiter, 2001). Heat advection in an inclined layer causes differences in vertical heat flow above and below the strata boundaries (Ziagos and Blackwell, 1981).

Vertical heat flow logs calculated from measured temperatures with such discontinuities indicate strata-bound heat advection. These variations are observed where the boreholes intersect regional aquifers or fault structures. Unknown variations in thermal conductivity may result in similar discontinuities in the calculated heat flow profile. Thus, they are source of error and misinterpretation. Under favorable conditions, however, magnitude and direction of the average Darcy flow can be estimated from the associated offsets in vertical heat flow profiles from different boreholes.

The approach was tested on data from two different sites in northern and southern Germany. In both case studies, both high-precision temperature logs and the required thermophysical properties were available. They differ, however, substantially with respect to data distribution and flow regime. As the presented method is sensitive to these conditions, results of different quality were obtained. One analysis (Section 3.2) suffering from unfavorable conditions with respect to number and distribution of temperature logs yields only a minimum estimate of the regional groundwater flow's magnitudes; the direction of flow remains unknown. The second example (Section 3.3) provides more information. Here, the flow direction was deduced from additional, independent information. This allowed to determine the Darcy flow along the flow path. Additionally, a synthetic example shows the full potential of the method for delivering both magnitude and direction of Darcy flow (Section 3.4).

3.1 Theoretical background

Fluid flow in sedimentary basins is often focused along thin horizontal permeable layers, and the normal flow component v_z may be assumed to be small compared to the horizontal component v_x. For this configuration an equation corresponding to Eq. (2.12) can be derived (Stallman, 1963; Reiter, 2001):

$$\frac{\partial^2 T}{\partial z^2} = \frac{(\rho\, c)_f}{\lambda_b}\, v_x\, \frac{\partial T}{\partial x}\,. \tag{3.1}$$

For a inclined layer, the direction parallel to the flow (index *l*) replaces the horizontal direction *x*:

$$\frac{\partial^2 T}{\partial z^2} = \frac{(\rho\, c)_f}{\lambda_b}\, v_l\, \nabla_l T. \tag{3.2}$$

Observing the definition of specific heat flow q (Eq. 2.2), the second derivative in Eq. (3.2) can be approximated by

$$\frac{\partial^2 T}{\partial z^2} \approx -\frac{\Delta q_z}{d\,\lambda_b}, \tag{3.3}$$

where Δq is the difference in vertical specific heat flow above and below the aquifer of thickness d. This approximation is valid for small inclinations α (Fig. 3.1), where

$$\frac{\partial T}{\partial z} \approx \frac{\partial T}{\partial n}, \tag{3.4}$$

with n being into the direction perpendicular to the layer. If α is larger than a few degrees, the assumption for Eq. (3.4) is violated not only for geometrical reasons: Hor-

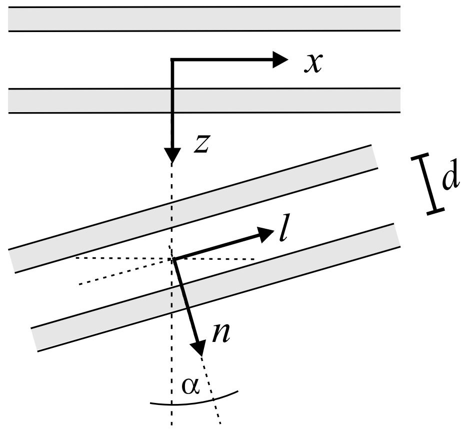

Fig. 3.1: Coordinate system where the z-axis is vertical and the x-axis is horizontal. For slopping aquifers this system is rotated, with the l-axis in the dip direction in the pane of the payer, and the z-axis normal to it.

izontal components of heat flow become also important as, in general, thermal conductivity will vary between the high-permeability layer and the surrounding rock. This is indicated by spikes in the heat flow profile along the borehole at material boundaries with abrupt changes in thermal conductivity. Inserting Eq. (3.3) into Eq. (3.2) we obtain:

$$\frac{\Delta q_z}{d} = -(\rho c)_f \; v_l \cdot \nabla_l T, \tag{3.5}$$

from which v_l can be determined if the other quantities are known, in particular the temperature gradient $\nabla_l T$ in the layer along the bedding and the heat flow offset Δq_z. Here Δq_z corresponds to the net heating (or cooling) caused by fluid flowing along a layer which is not parallel to the isotherms. Thus, the method returns the thermally effective component of the flow vector, the one parallel to the temperature gradient. Being a projection of the flow vector onto the temperature gradient, this yields a minimum estimate of the Darcy flow magnitude.

In the most simple case, the mean gradient may be approximated locally by fitting a surface to temperatures observed in different boreholes. The gradient can then be obtained from the coefficients of the equation. With sufficient data more sophisticated estimation schemes (e.g., Billings et al., 2002 a, b) should be considered.

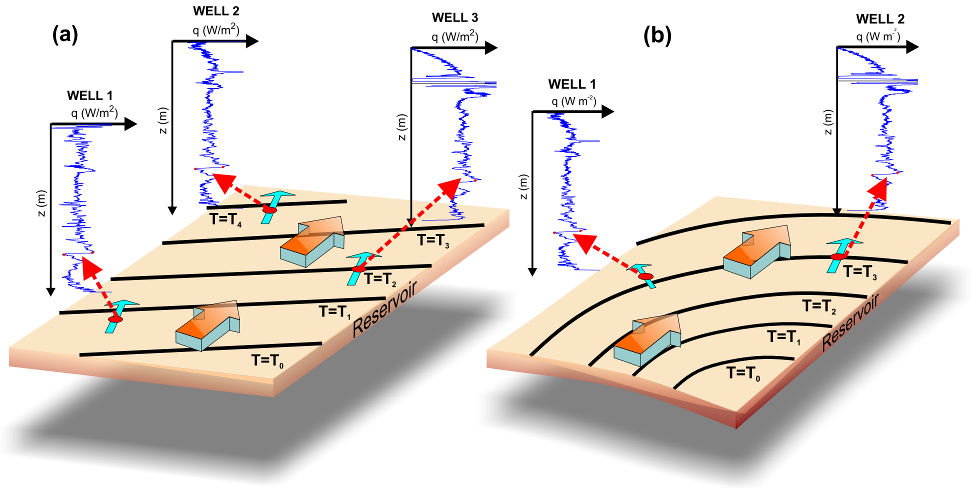

Fig. 3.2: Heat is advected by strata-bound groundwater flow (big arrows), creating an associated thermal signature in the vertical heat flow q (vertical profiles, well 1-3). Each offset in vertical heat flow is associated with a projection of the Darcy velocity onto the direction of temperature gradient (white arrows). (a) homogeneous direction of temperature gradient, yielding the same projection of the groundwater flow at every borehole resulting in a minimum estimate of groundwater flow. (b) variable directions of temperature gradient yielding different projections of groundwater flow at every borehole. At least two logs containing the characteristic thermal signature are necessary to derive both direction and magnitude of groundwater flow.

Unfortunately, in general the direction of the flow cannot be estimated if temperature is interpolated linearly by fitting a plane because this results in a constant temperature gradient in the flow domain (Fig. 3.2 a). However, more can be achieved if data from several boreholes are available and some more sophisticated approximation is employed to obtain a non-uniform temperature gradient in the flow domain. In this situation the efficiency of advective heat transport is variable and depends upon the angle between flow direction and temperature gradient. Therefore, we observe different thermal signatures in different boreholes. This may be interpreted as the effect of uniform mean flow projected onto a non-uniform temperature gradient (Fig. 3.2 b). In a similar way, the same effect might be caused by an inhomogeneous flow field projected onto a constant temperature gradient. However, as we consider regional flow fields, this scenario is less likely.

Values for Δq_z^i can be estimated for all boreholes and used in a least-squares estimation (e.g. Brandt, 1999) of the specific discharge vector's direction and magnitude. If we write Eq. (3.5) for each borehole, we will obtain an over-determined system of linear equations:

$$\frac{\Delta q_z^i}{d} = (\rho c)_f \cdot (v_{l,x} \nabla_{l,x}^i T + v_{l,y} \nabla_{l,y}^i T). \tag{3.6}$$

This system is solved for the unknown Darcy flow components in a least-squares sense. The advantage of this procedure is that it yields not only estimates of the flow magnitude, but also their statistical variance. Estimating the associated mean flow velocity $c = v/\phi$ requires additional information on porosity ϕ.

3.2 A case study from the Alpine Molasse Basin

The Alpine Molasse basin is an asymmetric foreland basin associated with the uplift of the Alps. It extends over more than 1000 km from Switzerland in the southwest to Austria in the northeast. The basin consists mainly of Tertiary sediments which were deposited from the Middle Oligocene to the Upper Miocene. The observed subsurface temperature field suggests advective perturbations to the generally conductive thermal regime. These are probably controlled by deeply penetrating vertical faults which provide local high-permeability vertical fluid pathways. In contrast, vertical Péclet number analyses on the same data in tectonically undisturbed sediments of the basin yield almost no flow. Numerous intercalations of low permeability clay- or siltstone in the *Lower Continental Molasse* stratigraphic unit impede vertical flow. The deeper *Baustein* beds dip gently to the southeast in the southwestern part of the *Upper Marine Molasse* unit. They are an important regional aquifer composed mainly of sandstones, which are partly cemented by carbonates (Kronmüller, 1987 a, b). The upper part of this layer is one of the major regional hydrocarbon reservoirs. It is effectively sealed at the top by the clay-rich *Upper Cyrenen* layer (Kronmüller, 1987 a, b). Below the *Baustein* unit, we find Jurassic limestones with several potentially karstic aquifers at deeper levels. They are of Middle Kimmeridgian to Lower Tithonian age (Bertleff et al., 1988), with local high permeability. These aquifers are considered to be responsible for most of the regional advective heat transport and therefore important for the understanding of the thermal regime.

For this study, continuous temperature logs with a sampling interval of less than 1 m were selected from a data base maintained at the Leibniz Institute for Applied Geosciences (GGA) in Hannover (Pribnow and Schellschmidt, 2000). They are considered to be free of technical perturbations due to drilling because their shut-in time before logging had been sufficiently long for a thermal equilibration. About 20 such temperature logs of up to a depth of 2000 m are available for the *Southern German Molasse Basin*.

In a first step, the logs were uniformly re-sampled at 1 m interval. Then, a paleoclimate signal was estimated by a joint inversion from a suitable subset of these data as described in Clauser and Mareschal (1995) and subtracted from each log. The paleoclimatic temperature signatures ΔT as well as the corresponding variations in vertical specific heat flow Δq are shown in Fig. (3.3) (Hartmann and Rath, 2005). The magnitude of the anomaly decreases with depth and reaches 2 K at the depth of the aquifer. The strata-bound analysis interprets abruptly changing vertical heat flow whereas the paleoclimate signatures has comparable small gradients. Thus, in general, the result of the strata-bound flow analysis is little affected by paleoclimate signatures.

After subtracting the paleoclimate signal from the temperature logs I calculated vertical temperature gradients from these reduced temperature logs and smoothed them using a moving average procedure. Finally, vertical heat flow profiles were calculated according to Eq. (2.2) using thermal conductivity measured on cores and derived from geophysical logs by an inverse estimation technique (Hartmann and Rath, 2005).

Heat flow logs which show a significant offset in vertical heat flow below and above permeable reservoirs were selected, and tested whether these offsets occur also in the same geological unit in logs from adjacent wells. A two-dimensional analysis requires at least three such logs. The observed signature can be attributed to strata-bound water flow with sufficient confidence provided that: (1) heat flow remains on different, more or less constant levels above and below the aquifer; a simple curved deviation from a constant vertical heat flow may imply an overlooked transient effect (Vasseur and

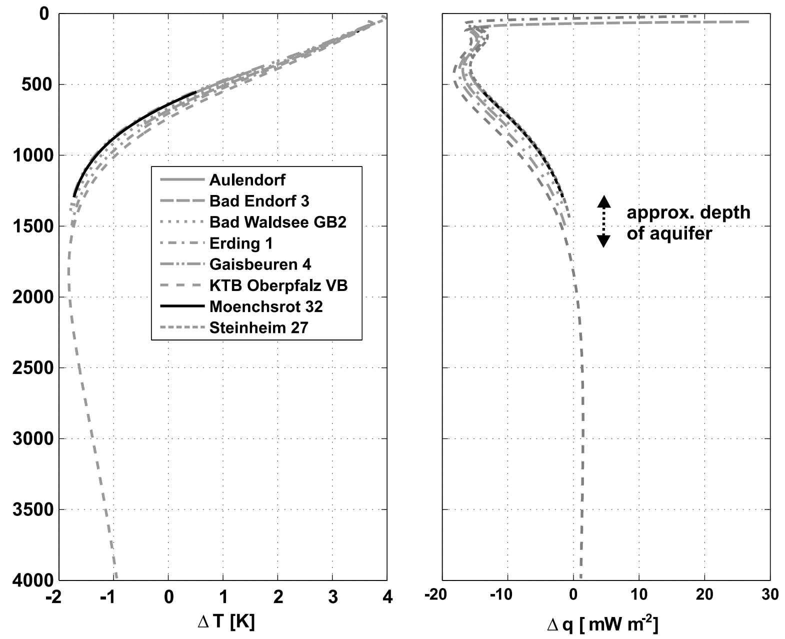

Fig. 3.3: Left panel: Paleoclimate signals inverted from several temperature logs from the *Southern Germany Molasse Basin*. Right panel: The corresponding anomaly of vertical heat flow (Hartmann and Rath, 2005). The black solid lines mark the result obtained for the logs of the study area.

Demongodin, 1995); (2) the variation in heat flow is larger than that which is due to the natural variation in rock thermal conductivity.

The reservoir properties of the *Baustein* beds are known to some extent (Kronmüller, 1987 a) and are favorable to potential groundwater flow due to high permeabilities of up to $10^{-12}\,\mathrm{m}^2$ (decreasing with depth). Three temperature logs sample this layer at a depth of about 1500 m below ground surface where they show an abrupt change in vertical heat flow (Fig. 3.4). The thickness of the reservoir is known from borehole records. The local temperature gradient along bedding in the layer was found by fitting a planar surface to the average temperature of the aquifer, yielding $23\ \mathrm{mK\,m^{-1}}$ at a direction of $164°$ from north. The velocity parallel to this gradient was assumed to be the mean value for the area between the boreholes which are a few kilometers apart. Thus, a homogeneous fluid flow can be assumed. The resulting minimum estimate of our analysis yields an average Darcy velocity of $2.6\ \pm\ 0.25\ \mathrm{m\,a^{-1}}$ for the *Baustein* beds (Fig. 3.5). Tab. (3.1) lists the parameters used in this analysis.

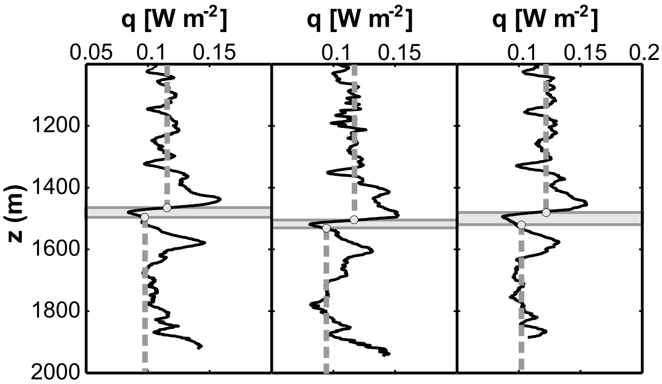

Fig. 3.4: Thermal signatures in the vertical heat flow logs at the depth of the *Baustein* beds reservoir. Δq is indicated by the offset of broken lines (Log 1 to 3 from left to right; see Tab. 3.1). Variations may be due to poorly resolved thermal conductivity.

Tab. 3.1: Parameter settings for the flow analysis in the Baustein beds.

	Easting (m)	Northing (m)	Δz (m)	Δq (Wm^{-2})	T $(°C)$
Log 1	3575960	5320855	34	0.024	65.4
Log 2	3574385	5319925	28	0.024	66.5
Log 3	3576000	5320730	42	0.032	65.7

3.3 A case study from the Dömitz-Lenzen syncline in northern Germany

The flow analysis in the previous example (Section 3.2) yielded a minimum estimate of the Darcy flow in the *Baustein* aquifer only. Lack of data prevented an analysis of the specific magnitude and direction of the flow. In the following example, available data and the geothermal situation alow to estimate the Darcy flow magnitude.

The Dömitz-Lenzen syncline is adjacent to the northern flank of the Gorleben salt diapir in the *Northern German Basin*. This diapir has an elongated shape, striking NE-SW and is composed of Upper Permian (*Zechstein*) evaporites. Its approximate length is 14 km, its width 4 km, and its base is at 3 km depth. During its ascent rim synclines evolved to the northwest and southeast, where Mesozoic and Tertiary sediments were accumulated to a thickness of about 300 m. Part of this formation is a known regional

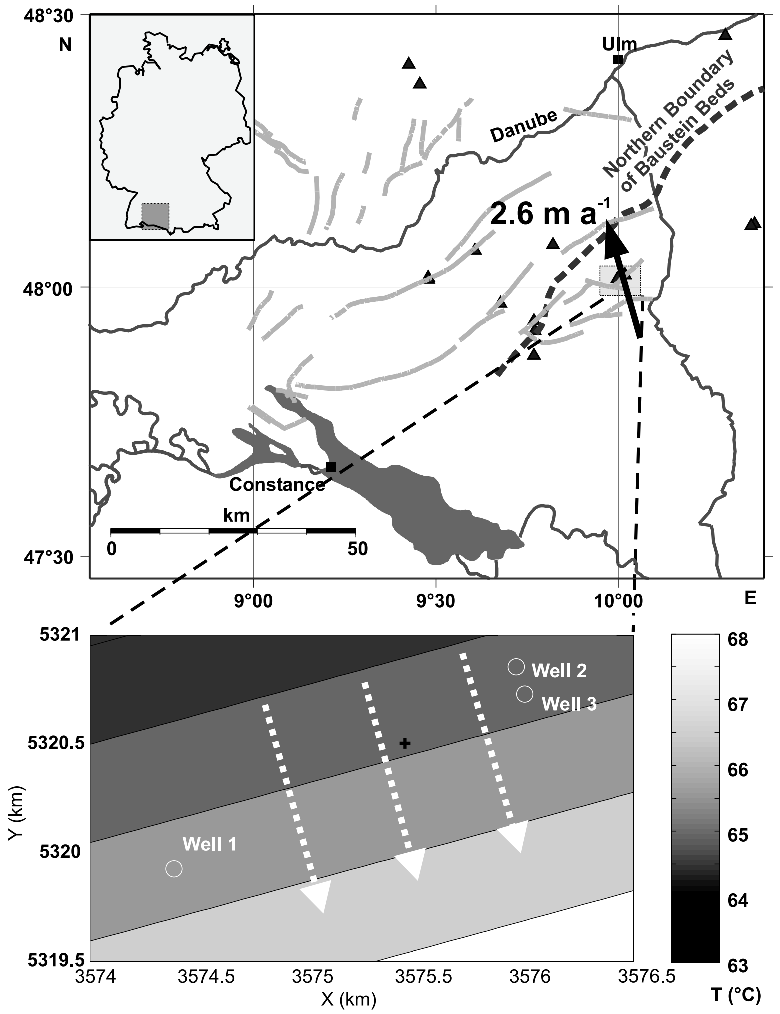

Fig. 3.5: Minimum estimate of regional strata-bound flow in the *Baustein* beds reservoir of the *Southern German Molasse Basin* at approximately 1500 m depth determined from heat flow logs in three boreholes. The minimum mean Darcy flow (black arrow, top panel) is $2.6 \pm 0.25\ \mathrm{m}\, a^{-1}$. The temperature gradient is directed $164°\mathrm{N}$ (white arrows, bottom panel). Triangles indicate locations of boreholes with temperature logs, gray lines are fault zones.

aquifer the *Miocene Lignite Sands* confined by the *Hamburg Clay* at the top and by Oligocene clays at the base (Klinge et al., 2002).

Subglacial erosion during the Elsterian glaciation (480 000 - 420 000 y.b.p.) eroded partly Tertiary clays on the top of the diapir and formed the N-S striking *Gorleben Erosion Channel*. The channel is filled by highly permeable Quaternary sediments which lie partly on top of the *Zechstein* salt. Towards the top this aquifer is confined by the

Lauenburg Clay. It is connected hydraulically to the *Lignite Sand* in both synclines.

In the past, this salt dome was explored in detail as a potential nuclear repository site. During exploration, many hydrogeological exploration and observation wells were drilled. Twenty-two of them fall within a region (Fig. 3.6) of active flow. In all of these wells temperature and salinity were measured (Schildknecht, 1999; Grissemann and Czora, 2003).

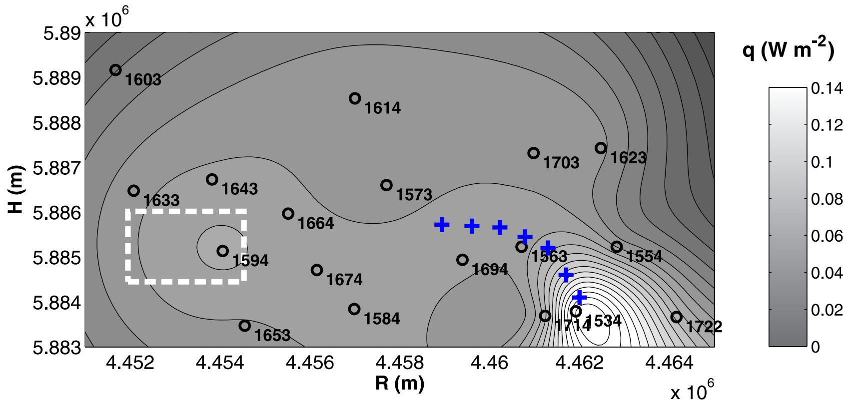

Fig. 3.6: Map of the specific vertical heat flow component calculated according Eq. (2.3) from temperature logs and thermal conductivity in the Gorleben area. Circles show the position of wells and temperature logs. The average specific heat flow of the lower section of each log was used for interpolation. The boxed area is assumed to be unaffected by advection. Here, the average specific heat flow is $62\ \mathrm{mW\,m^{-2}}$. Crosses indicate the flow path inferred from salinity data.

Salinity measurements in the Quaternary sediments detected anomalously high concentrations of $200\ \mathrm{g\,L^{-1}}$ up to $320\ \mathrm{g\,L^{-1}}$ at the base of the erosion channel, where the groundwater is in contact with the *Zechstein* salt. In contrast, the regional background value is about $0.2\ \mathrm{g\,L^{-1}}$. This anomaly extends from the channel to the northern rim syncline, $100\ \mathrm{m}$ below, showing that there is a hydraulic connection (Fig. 3.7). The solute content decreases to values of $10\ \mathrm{g\,L^{-1}}$ $30\ \mathrm{g\,L^{-1}}$ in the syncline. This observation is explained by groundwater flow driven by both density and topography (Klinge et al., 2002). Moreover, the salinity measurements show that the flow does not involve the full vertical interval of the aquifer. Rather, the high-density brine flows below a layer of lighter fresh water.

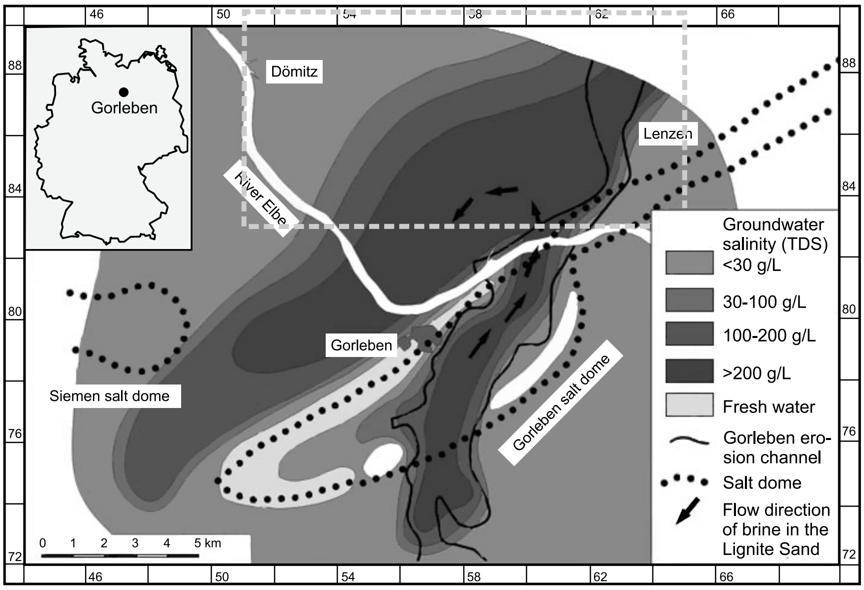

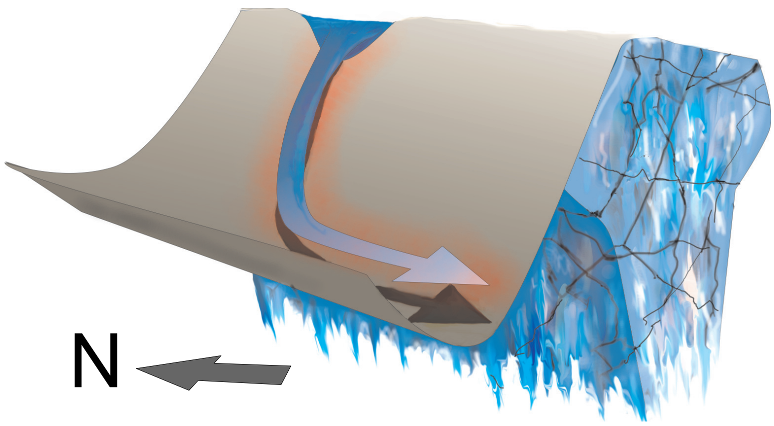

Fig. 3.7: Top panel: Salinity map of the Dömitz-Lenzen area in northern Germany (Klinge et al., 2002, modified). The groundwater flow from the erosion channel on top of the salt dome into the rim syncline is deduced from the salinity anomaly. The study area is outlined by the dashed box. Bottom panel: Illustration of the flow path accompanied by a thermal anomaly.

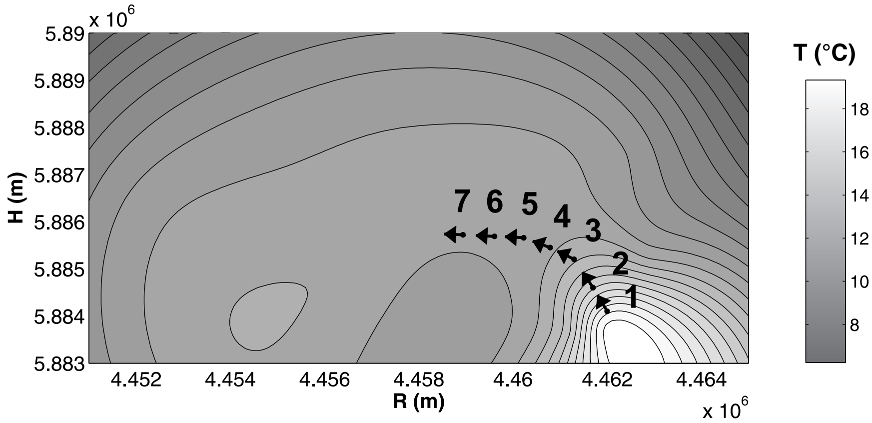

Fig. 3.8: Interpolated temperature map at -160 m a.s.l.. Arrows indicate the assumed flow path, their length is proportional to the calculated Darcy flow. The assumed flow path follows a declining temperature anomaly in the south east bending into the direction of the depression. Numbers correspond to logs in Tab. (3.2).

Apart from the salinity anomaly the flow is accompanied by a considerable temperature and heat flow anomaly (Fig. 3.8). For reasons beyond my control, temperature was not measured sufficiently deep to sample directly the fluid flow at the bottom of the syncline. To obtain expressions for $\nabla_l T$ in Eq. (3.5), $\partial T/\partial x$, $\partial T/\partial y$, and $\partial T/\partial z$ had to be extrapolated down to the horizon of interest 50 m - 100 m below. The vertical temperature gradient (Fig. 3.9) seems to vary little. For the flow analysis the gradient at the bottom of each log was projected to the depth of groundwater flow. The profiles in Fig. (3.9) reflect a decreasing magnitude of the horizontal temperature gradient along the flow path nearly vanishing at its end. Since flow distorts temperature distribution, the true gradient within the flow domain might be different. According to Eq. (3.5) the flow would be over-estimated if the gradient is under-estimated.

The vertical heat flow component is calculated from synthetic logs of thermal conductivity derived from wireline logging (Grissemann and Czora, 2003) and vertical temperature gradients according to Eq. (2.2) (Fig. 3.10 and Fig. A.1 in the Appendix).

An average value of the lower portion of each log was used for the interpolation of a heat flow map (Fig. 3.6). The specific heat flow should be on a constant level because this is an indication for good resolved thermal rock conductivity and the absence of disturbing effects. Given that, this interval represents the specific heat flow which is

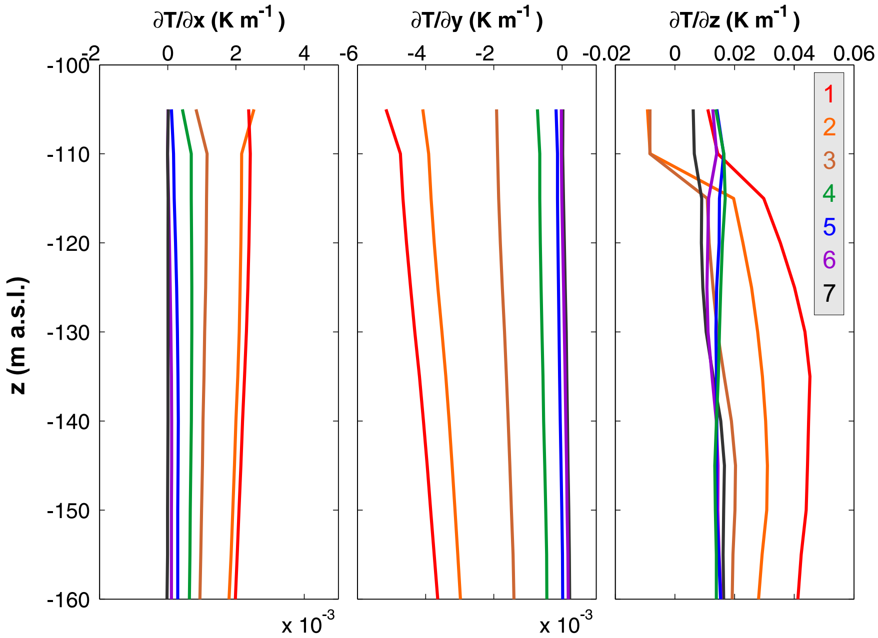

Fig. 3.9: Logs of temperature gradient in components x-, y- and z-direction at each location listed in Tab. (3.2) and shown in Fig. (3.8). The color code indicates the log numbers (Tab. 3.2). All three plots show that the temperature gradient decreases along the flow path nearly vanishing at the end.

passed vertically from the layers below to the surface by conduction. In the heat flow map (Fig. 3.6) a clear anomaly can be seen which is attributed to the heat advected on the lower horizon of the aquifer. The anomalous high temperature in the flow domain induces an increased specific heat flow in the layers above.

To obtain Δq for Eq. (3.5) a background value considered to be due to thermal diffusion only, needs to be subtracted from the vertical heat flow. The residual component then characterizes the advective part of heat transfer, Δq. In this case, the background value is estimated to be $62\ \mathrm{mW\,m^{-2}}$ in the area unaffected by the flow to the west (box in Fig. 3.6). The diapir has a comparatively high thermal conductivity which focuses heat flow along the structure. This results in a decreased regional heat flow around the diapir. To account for this influence the background value is determined at a position equally far from the salt dome as from the flow region (see Fig. 3.6 and 3.8).

A flow path could be inferred from an analysis of the underground structure and the distribution of salinity (crosses in Fig. 3.6). At each location the flow was calculated according to Eq. (3.5). It is assumed that the flow is parallel to the base of the aquifer being approximately -210 m a.s.l. on top of the diapir and -260 m a.s.l. in the synlcine.

A vertical thickness of d $\approx$ 30 m was inferred for the flow system from salinity logs. This is possible because the flow is associated with elevated salinity. Results of each flow estimate are listed in Tab. (3.2). They are consistent with a continuous flow yielding an average magnitude of $|v| = 2.1\ \mathrm{m\,a^{-1}}$. Assuming a porosity of 10 % - 20 % this yields a flow velocity in the range $10\ \mathrm{m\,a^{-1}}$ - $20\ \mathrm{m\,a^{-1}}$. This result agrees with the conclusion of Klinge et al. (2002) who give a range of possible flow velocities from $1.5\ \mathrm{m\,a^{-1}}$ to $250\ \mathrm{m\,a^{-1}}$ for near-surface aquifers in this area.

Tab. 3.2: Results of the flow analysis in the Gorleben area. The location of each log with the coordinates *x* and *y* are shown in Fig. (3.6).

Log	x (m)	y (m)	azimuth (°)	dip (°)	v_f $(m\ a^{-1})$
1	4462000	5884100	-31	-13.0	2.03
2	4461700	5884600	-34	-9.0	2.11
3	4461300	5885200	-64	-6.5	2.12
4	4460790	5885450	-69	-4.5	2.13
5	4460230	5885660	-87	-3.0	2.19
6	4459610	5885690	-87	-2.7	2.08
7	4458940	5885720	-87	-2.3	2.13

3.4 Synthetic example

Since no fully complete set of field data is available at present, I use a synthetic temperature field to demonstrate the full potential of this approach. A numerical three-dimensional simulation with a commercial finite element code[1] illustrates the thermal effect of steady-state, strata-bound fluid flow on temperature and heat flow logs. From these synthetic data hypothetical temperature logs where extracted and analyzed as explained above. Under these ideal conditions, both magnitude and direction of the

[1]FEFLOW® Wasy GmbH, Berlin; http://www.wasy.de

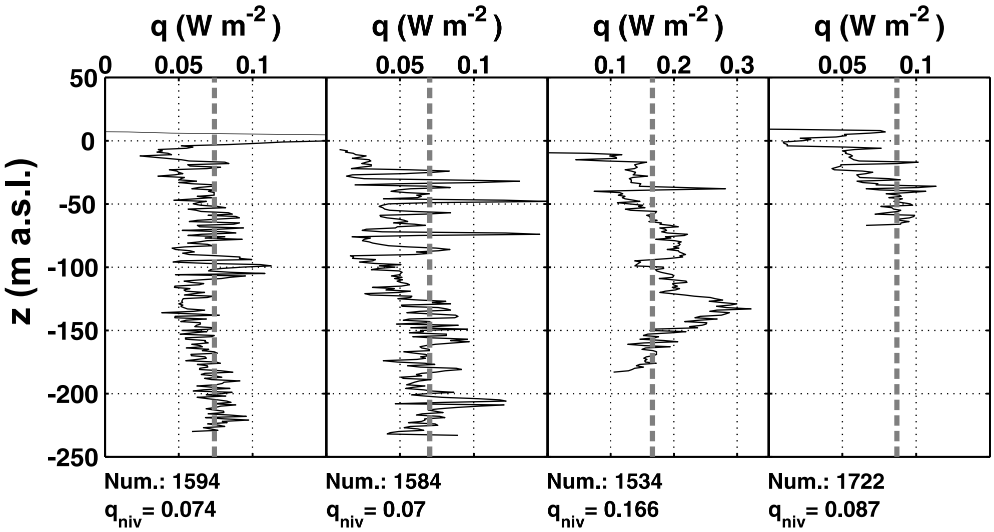

Fig. 3.10: Logs showing anomalously high heat flow. Logs of average heat flow are found in the Appendix (A.1). q_{niv} is the average heat flow at the lower part of the logs (broken lines). The difference between q_{niv} and the background value of $62\ \mathrm{mW\,m^{-2}}$ is attributed to heat advection. The numbers at each log indicate the borehole location in Fig. (3.6).

mean flow vector in the aquifer can be obtained as well the associated errors.

Fig. (3.11 a) shows an inclined, high-permeability ($10^{-11}\,\mathrm{m^2}$) layer of concave topography in an otherwise conductive temperature field. A small hydraulic gradient of 4×10^{-4} is due to constant hydraulic heads (2 m and 0 m) at the front and rear boundaries, respectively (horizontal distance: 5 km). It drives warm water along the permeable layer up-dip into colder regions with a Darcy velocity of $1.21\ \mathrm{m\,a^{-1}}$ - $1.26\ \mathrm{m\,a^{-1}}$. This results in different angles between the temperature gradient and the flow vector. The permeability k of the homogeneous host rock is $10^{-14}\ \mathrm{m^2}$. There is no heat production, and thermal conductivity is uniform and constant at $3\ \mathrm{W\,m^{-1}K^{-1}}$ throughout the model. At the top of the model temperature is constant at $\mathrm{T_0} = 10\,^\circ\mathrm{C}$, and a constant vertical specific heat flow of $60\ \mathrm{mW\,m^{-2}}$ enters at the bottom. The efficiency of the advective heat transfer varies with the angle between the flow vector and the temperature gradient. Hypothetical vertical temperature logs were extracted along the dashed lines marked in Fig. (3.11 b). They are shown together with the corresponding vertical heat flow logs in Fig. (3.11 c). These logs indicate the thermal effect of strata-bound heat advection by a vertical temperature gradient which is larger above the aquifer than below. Since thermal conductivity is constant, vertical heat flow varies accordingly across the aquifer. The observed variations in vertical heat flow are due to the varying angle between flow direction and temperature gradient, which determines the amount of net heat advected in the layer (Δq in Tab. 3.3). Applying this method to extracted synthetic temperature logs we obtain an estimate of the magnitude and direction of the mean fluid flow vector (Fig. 3.11 d). Five synthetic logs were used in the analysis and yield Darcy velocities shown in Tab. (3.4). In the example the aquifer thickness was derived from the thermal signature as well as Δq. Thus, both are sensitive to log interpretation. Simulated and analyzed flow directions deviate only by $1.6\,^{\circ}$. In fact, the flow path is not always parallel to the lateral boundaries of the model. Obviously, the accuracy of the analysis depends strongly on the selected temperature logs. For instance, the results will be unreliable if estimates are based on projections on collinear gradients.

Tab. 3.3: Modelled parameters of each borehole for a least-squares estimation of Darcy flow.

Log	h (m)	Δq (Wm^{-2})	T_{mean} $(^{\circ}C)$	$\nabla_{l,x}T$ (Km^{-1})	$\nabla_{l,y}T$ (Km^{-1})
1	74	0.060	50.41	0.0066	0.0046
2	66	0.050	51.07	0.0055	0.0060
3	68	0.034	48.36	0.0035	0.0077
4	72	0.018	43.31	0.0019	0.0085
5	70	0.01	39.71	0.0011	0.0085

Tab. 3.4: Mean Darcy velocities in synthetic example (Fig. 3.11).

	$v\ (m\,s^{-1})$	$v\ (m\,a^{-1})$
Simulated	3.904×10^{-8}	$1.21 - 1.26$
Analyzed	3.313×10^{-8}	1.05

Due to the shape (varying dip) of the aquifer, flow paths have different lengths ranging from 5000 m - 5220 m. According to Darcy's law (Eq. 2.10), this yields velocities of $1.21\ \mathrm{m\,a^{-1}}$ - $1.26\ \mathrm{m\,a^{-1}}$ (Tab. 3.4). Assuming standard values for water density of $\rho_\mathrm{f} = 1000\ \mathrm{kg\,m^{-3}}$ and dynamic viscosity of $\mu = 10^{-3}\ \mathrm{Pa\,s}$, the analysis yields a flow magnitude which is 14 % - 17 % too low compared to the simulation results.

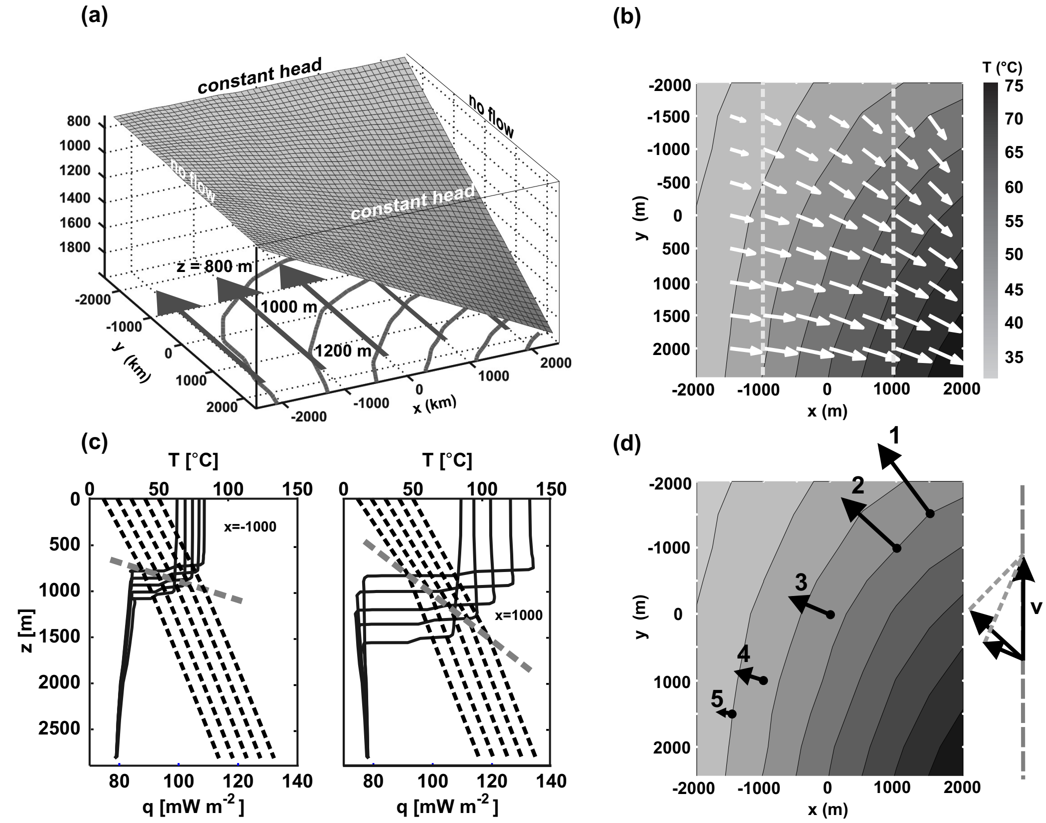

Fig. 3.11: Synthetic example (a): In an inclined high permeable layer in a low-permeable host rock a constant hydraulic gradient drives an up-dip flow field (black arrows). (b) The geometry of the aquifer leads to a variable temperature field within the aquifer (filled isolines). White arrows show the temperature gradient. Dashed lines mark the x-coordinate of the logs shown in the next panel. (c) Temperature and heat flow logs (dotted and solid lines, respectively) calculated at five different positions along the two dashed lines in panel (b). The thick, broken gray line indicates the depth where the logs intersect the aquifer. (d) Projections of groundwater flow onto the temperature gradient (logs 1-5 in Tab. (3.3)).

Chapter 4

Correction of non-equilibrated temperature logs

Accurate information about the thermal regime is the base of any geothermal analysis. If temperature logs are to be used for estimating flow or other temperature sensitive quantities, they need to be as accurate as possible. During the drilling process, drill mud is circulated in the drill string and the annulus to carry cuttings out of the borehole. Correspondingly, heat is advected along the borehole and exchanged laterally with the formation. As a result, the host rock is either heated or cooled. This transient thermal perturbation results in a characteristic curved, temperature signature in the temperature log.

Heat advection by fluid flow introduces curvature in a temperature log as well as diffusion of transient variations of ground surface temperature. Péclet number analysis (Bredehoeft and Papadopulos, 1965; Clauser, 1988), for instance, interprets the curvature of a temperature log as an effect of steady-state groundwater flow. For non-equilibrated temperature logs this analysis will be in error. Often, the maximum temperature in a borehole would be under-estimated. Therefore, potential areas for exploration of geothermal energy would appear less favorable. Temperature measurements are performed best after a sufficiently long shut-in time when the influence of mud circulation has faded away and the equilibrium formation temperature has been reached. For economic reasons, this is often not possible in commercial boreholes. If this technical disturbance is ignored, however, this signature signal may be misinterpreted and attributed, for instance, to groundwater flow.

With regard to the large number of data available from the petroleum industry it is not surprising that methods are available for estimating the undisturbed formation temperature from technically disturbed data. Horner's method (Horner, 1951; Lachenbruch and Brewer, 1959; Dowdle and Cobb, 1975) is an analytical approach that requires transient temperature records during the shut-in phase. It is frequently applied to bottom hole temperatures (BHT). Other methods are based on inversion (Tarantola and Valette, 1982) or stochastic inversion techniques (i.e. Vasseur et al., 1985). Kutasov (1999) assessed quantities which result from the drilling process, such as radial heat flow between borehole and formation.

In the following, I present a novel correction technique combining the principle of super-position with estimates of radial heat flow along the borehole. The approach requires only a single temperature log. For validation it is applied both to synthetic data from numerical simulations and to equilibrated and non-equilibrated temperature logs from the same borehole. Further, I discuss whether corrected non-equilibrated data can be used for the analysis of steady-state subsurface fluid flow and the variations of the Earth's ground surface temperature in the past.

4.1 Theoretical background

If heat generation and advection are neglected, Eq. (2.11) for transient diffusion of heat simplifies to

$$(\rho\, c)_b \frac{\partial T}{\partial t} = \nabla \cdot (\lambda_b\, \nabla T)\,. \tag{4.1}$$

By setting the conditions to

$$\begin{array}{ll} t \leq 0\text{:} & T(r,t) = T_0, \\ t \geq 0,\ r = 0\text{:} & \lim_{r\to 0}(r\frac{\partial T}{\partial r}) = -\frac{q_h}{2\pi\lambda}, \\ t \geq 0,\ r = \infty\text{:} & T(r,t) = T_0, \end{array}$$

the solution of the differential equation for an infinite line source in a radially infinite space can be written as (Carslaw and Jaeger, 1959, p. 261):

$$\Delta T(r, t_c) = \frac{q_h}{4\pi\lambda} \cdot E_1\left(\frac{r^2}{4\kappa t}\right) \quad \text{where} \quad E_1 = \int_x^\infty \frac{e^{-t}}{t}\, dt \tag{4.2}$$

is the $\mathrm{E_n}$-function for $\mathrm{n} = 1$ which is related to the exponential integral

$$E_i(x) = -\int_{-x}^\infty \frac{e^{-t}}{t}\, dt \quad \text{by} \quad E_1(x) = -E_i(-x)\,. \tag{4.3}$$

Here, t is time (s), κ thermal diffusivity ($\mathrm{m^2\,s^{-1}}$), q_h horizontal, radial heat flow ($\mathrm{W\,m^{-1}}$) and r (m) is the distance normal to the line source.

Horner's method applies the line source model for extrapolating the transient equilibration process. Therefore, it is only applicable if a time series of shut-in time temperatures is available. Then t_c is then the time of exposure of the rock to the circulating mud. It is controlled by the drilling rate and therefore varies with depth z.

The principle of super position (Bullard, 1947) will apply if different time intervals of different radial heat flow have to be considered. In the present case there are two: the circulation time t_c and the subsequent shut-in time t_s. The shut-in phase is accounted for by an additional term in Eq. (4.2):

$$\Delta T(r, t_c, t_s) = \frac{q_h}{4\pi\lambda} \cdot \left\{ \underbrace{E_1\left[\frac{r^2}{4\kappa(t_s + t_c)}\right]}_{circulation} - \underbrace{E_1\left[\frac{r^2}{4\kappa t_s}\right]}_{shut-in} \right\}. \tag{4.4}$$

For reconstruction of borehole temperatures, r is the borehole radius. This solution (Bullard, 1947) corresponds to the theory for the analysis of hydraulic well testing (Theis, 1935). Its general characteristic is shown in Fig. (4.1). The mathematical model implies an infinite equilibration time to undisturbed formation temperature. However, there will be a time after which the residual becomes negligible.

The radial, horizontal heat flow from the borehole into the formation ($q_h(z)$) is mainly controlled by the difference between mud temperature $T_m(z)$ and formation temperature $T_f(z)$. Due to the increasing borehole depth the temperature of the mud

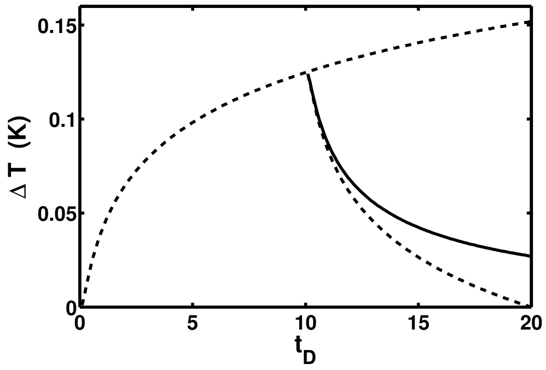

Fig. 4.1: The nature of a heating and subsequent cooling process induced by a line source. Plotted is ΔT versus the dimensionless time $t_D = \kappa\ t/r^2$. The two broken curves are calculated from Eq. (4.2) for circulation $(tc + ts)$ and shut-in (t_s). The solid curve is obtained by superponing circulation and shut-in according to Eq. (4.4).

increases according to the formation temperature gradient but introducing an adapted circulation time permits to identify the temperature with the constant *apparent temperature of the heater*. Several authors demonstrated (Lachenbruch and Brewer, 1959; Jaeger, 1961; Edwardson et al., 1962; Ramey, 1962; Raymond, 1969) that this simplification is applicable for boreholes up to $5000\ \mathrm{m}$ depth. Kutasov (1999) estimates radial heat flow from formation and mud temperatures, T_f and T_m, respectively:

$$q_h = 2\pi\lambda \cdot (T_f - T_m) \cdot q_D(t_D). \tag{4.5}$$

Here, the dimensionless time is

$$t_D = \frac{\kappa t_c}{r^2} \tag{4.6}$$

and in analogy the adapted, dimensionless time is

$$t_D^* = \frac{\kappa t_c^*}{r^2}\ . \tag{4.7}$$

Kutasov (1999) distinguishes two cases:

$$t_D \leq 10: \qquad t_D^* = t_D \left[1 + \frac{1}{1 + \frac{7}{8}\ln(1+t_D)^{\frac{2}{3}}}\right], \tag{4.8}$$

$$t_D > 10: \qquad t_D^* = t_D \left[\frac{\ln t_D - \exp(-0.236\sqrt{t_D})}{\ln t_D - 1}\right]. \tag{4.9}$$

Dimensionless heat flow is described by

$$q_D = \frac{1}{\ln(\frac{\pi}{2} + \frac{1}{\sqrt{t_D}+\sqrt{\pi}-\frac{\pi}{2}}\sqrt{t_D})}. \tag{4.10}$$

Rather than extrapolating Eq. (4.4) to infinite time based on a time series of repeat temperature measurements the novel technique proposed here combines the principle of superposition of the line-source model (Eq. 4.4) and the estimates of radial heat flow (Eq. 4.5). Subsequent temperature measurements are therefore not required. Inserting Eq. (4.5) into Eq. (4.4) yields

$$\Delta T(r, t_c, t_s) = \frac{(T_f - T_m)\cdot q_D(t_D)}{2} \cdot \left\{E_1\left[\frac{r^2}{4\kappa(t_s+t_c)}\right] - E_1\left[\frac{r^2}{4\kappa t_s}\right]\right\}. \tag{4.11}$$

The parameters t_c, t_s, T_f and T_m are functions of depth (z in m). Times t_s and t_c can be inferred from the drilling history. Equation (4.11) describes then the temperature disturbance ΔT at any depth and can thus be determined for every depth point of the temperature log. This requires that a function $T_f(z) - T_m(z)$ is defined. Assuming a linear variation of $T_f(z) - T_m(z)$ with depth (Fig. 4.2) permits to interpolate over the entire log interval if at least two data points are available. These can be taken e.g. from BHTs and surface temperatures derived from climatological data. Surface temperatures can also be inferred from temperature logs measured in adjacent wells.

4.2 Correction of synthetic temperature logs

For verification the novel technique is applied to synthetic data. Contrary to field data, these are free of unknown, biasing effects such as lateral influx of groundwater into the borehole, variations of thermal rock properties and uncertainties regarding the

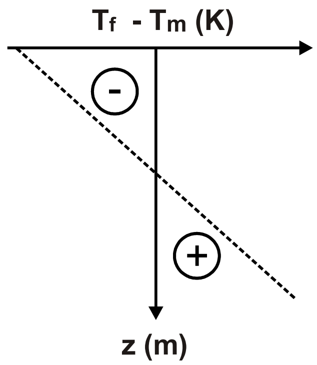

Fig. 4.2: Assumed linear variation with depth of the difference between formation temperature T_f and mud temperature T_m for use in Eq. (4.11).

drilling history. 2D numerical simulations based on finite differences were performed which consider the increase of borehole's depth, the mud circulation in the drill string and in the annulus, as well as the thermal properties of the rocks and the casing. The software code BOA (Kessels, 1988) was specifically designed for this purpose and permits to calculate transient processes which are radially symmetrical with respect to the borehole axis.

Tab. 4.1: Model settings for three scenarios considered.

	model a	model b	model c
number of layers	1	3	3
layer 1 (λ in $\mathrm{W\,m^{-1}K^{-1}}$, depth in m)	3, 1000	4, 300	2, 300
layer 2 (λ in $\mathrm{W\,m^{-1}K^{-1}}$, depth in m)	-	1, 600	3, 600
layer 3 (λ in $\mathrm{W\,m^{-1}K^{-1}}$, depth in m)	-	4, 1000	2, 1000
mud temperature at the top	time dependent	10 °C	10 °C
diameter of the casing	$12.7\,\mathrm{cm}$		
drilling rate	$1.375\ \mathrm{m\,h^{-1}}$		
temperature at the top	$10\ °\mathrm{C}$		
initial temperature gradient	$30\ \mathrm{K\,m^{-1}}$		
mud circulation rate	$300\,\mathrm{l\,min^{-1}}$		
heat generation by friction	none		

Tab. (4.1) lists the parameters of three simulated scenarios. They were held constant throughout the simulation time unless otherwise noted. The maximum depth is $1000\ \mathrm{m}$, the vertical node spacing is 1 m, and the drilling requires 30 days.

Following shut-in, the equilibration of the disturbed temperature (i.e. the initial temperature in the simulation) begins and is observed over two months of simulation time. The injection temperature of the mud entering into the top of the borehole is a function of time in model (a). It corresponds to the average formation temperature of the penetrated interval, increasing linearly from $10\,^{\circ}\mathrm{C}$ to $25\,^{\circ}\mathrm{C}$. Model (b) and (c) have a stratified subsurface and a constant injection temperature of $10\,^{\circ}\mathrm{C}$. The results of model (a) are shown in Fig. (4.3) and the evolution of the borehole temperature of the three models in Fig. (4.4).

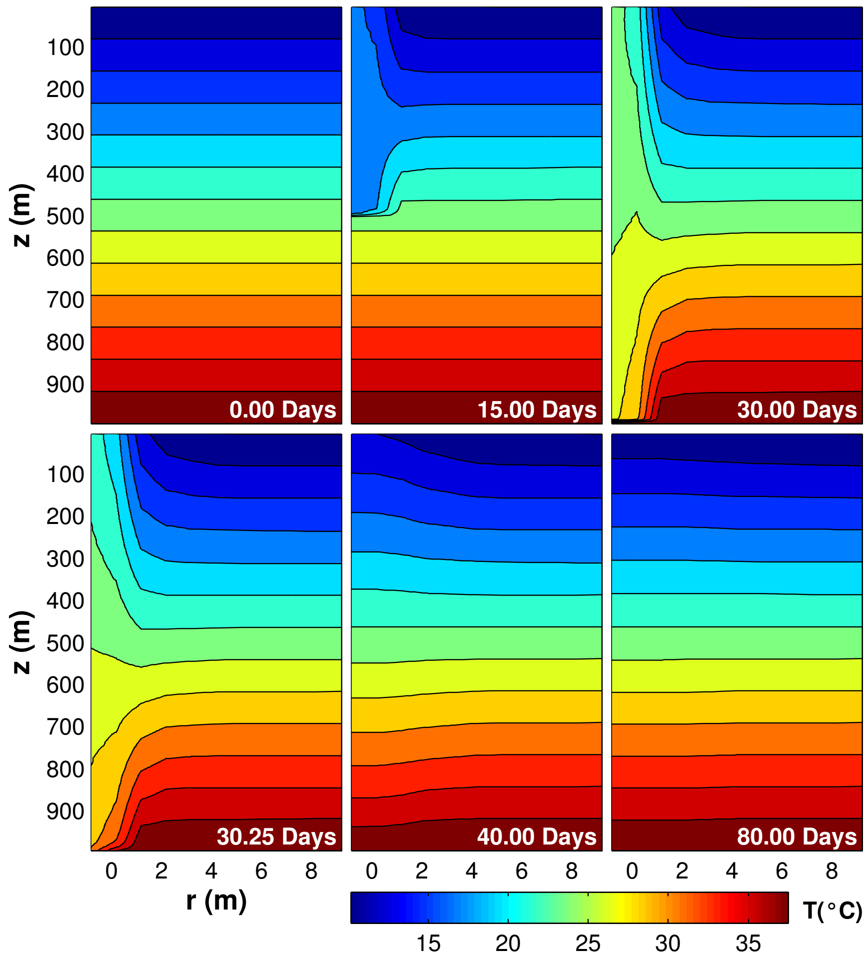

Fig. 4.3: Transient temperature distribution for model (a). The cross sections show depth (z) versus radial distance to the borehole (r). The mud is circulated for 30 days while the borehole depth increases. After shut-in, the temperature of the host rock equilibrates.

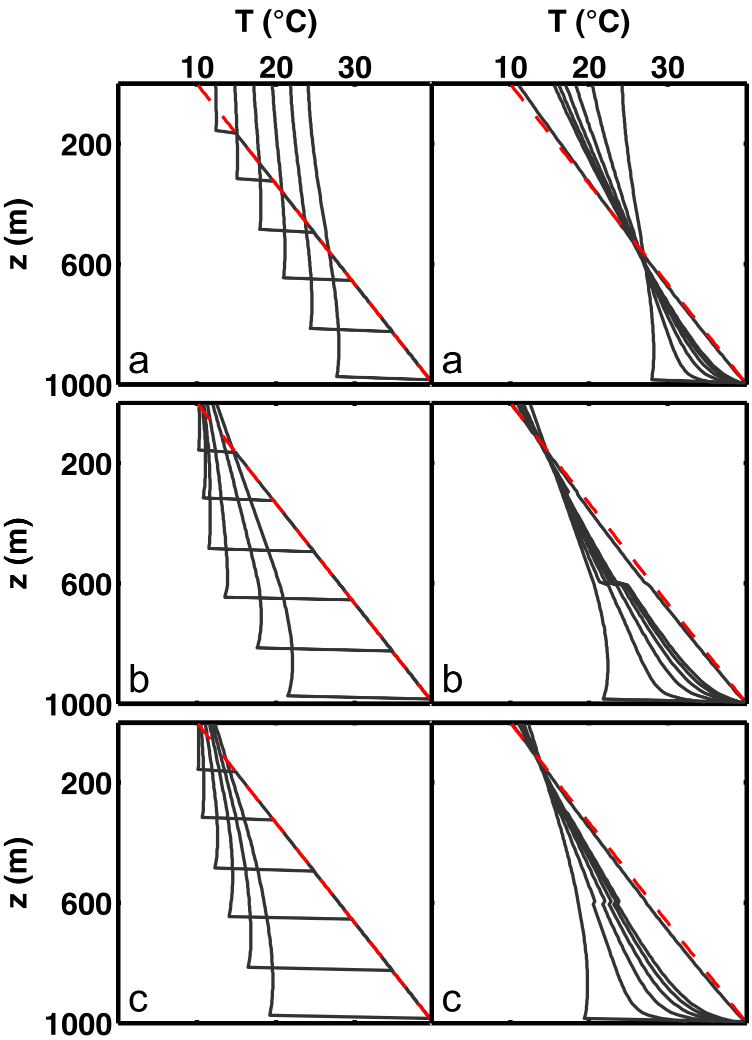

Fig. 4.4: Temperature logs for models *a*, *b*, and *c*. The shown temperature logs during circulation phase (left column) are at time intervals: 5, 10, 15, 20, 25, and 30 days, from left to right. The selected shut-in times (right column) are: 30, 30.5, 31, 31.5, 32, 32.5 and 60 days, from left to right. Note that the equilibration of the borehole temperature begins after 30 days. The broken line is the equilibrated temperature log.

Eq. (4.11) was solved for each sampling point yielding the function $\Delta T(z)$. Parameters such as thermal conductivity, thermal diffusivity and casing diameters correspond to the input parameters of the models. Shut-in and circulation times $t_s(z)$ and $t_c(z)$, respectively, were derived from the drilling history. The correction procedure was applied to temperature logs with 15 days of shut-in time by subtracting the correction function $\Delta T(z)$ from the non-equilibrated logs and comparison with the equilibrated temperature. The apparent horizontal heat flow q_h from the line-source is adjusted by the iterative modification of the term $T_f(z) - T_m(z)$ in Eq. (4.5) until the residual between the corrected temperature and the formation temperature is minimized.

Fig. (4.5) shows the results of a correction on synthetic data (models a, b and c). The best results were obtained for the correction of the log from model (a). The correction of logs from the scenarios with stratified subsurface show larger errors. The largest mismatch is observed at the bottom of the borehole because the infinite line-source model is inadequate near the bottom of a finite borehole. Generally, the difference between the equilibrium temperature and the corrected temperature log is less than 0.25 K.

4.3 Correction of recorded temperature logs

Several temperature logs from boreholes in *Brandenburg* nearby *Berlin* in Germany are suitable for testing the correction method with respect to the thermal disturbance by drilling and mud circulation. They were logged when both equilibrated and non-equilibrated. Thermal conductivity and diameter of the casing are unknown and therefore uniformly set to $3\ \mathrm{W\,m^{-1}K^{-1}}$ and $12.7\,\mathrm{cm}$, respectively. As in the example with synthetic data, the term $T_f(z)-T_m(z)$ in Eq. (4.5) was adjusted until the difference between the corrected temperature and the formation temperature was minimized. The resulting horizontal heat flow can be regarded as an effective heat flow affected by the above made assumptions concerning borehole diameter and thermal conductivity. Despite the unknown variation in thermal conductivity, the general trend is fitted well (Fig. 4.6). Small variations of the temperature log are not resolved but the accuracy is mostly better than 0.5 K.

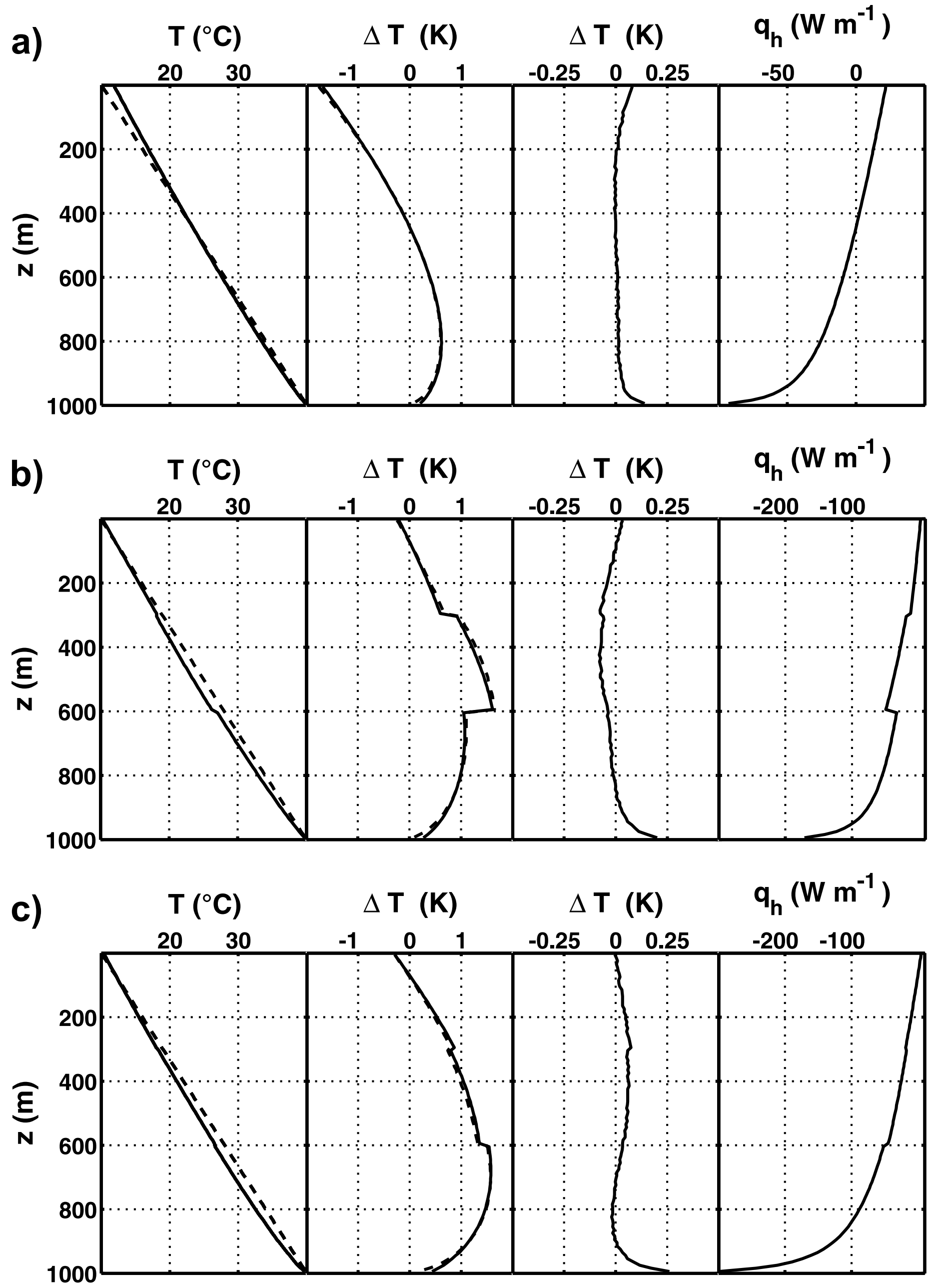

Fig. 4.5: Results of a correction applied on synthetical temperature logs. Model a: homogeneous subsurface with a thermal conductivity of $3\ \mathrm{W\,m^{-1}K^{-1}}$. Model (b) and model (c): subsurface is compound of three layers with a thermal conductivity of 4, 1, $4\ \mathrm{W\,m^{-1}K^{-1}}$ and 2, 3, $2\ \mathrm{W\,m^{-1}K^{-1}}$, respectively. Explanation of plots from left to right: First plot, dashed lines are the disturbed temperature logs depicted together with the initial or formation temperature, solid line. Solid lines on the second plot show the calculated correction function which is added to the disturbed temperature for a correction. These curves lie almost completely on top of the dashed curves, the true correction functions. The third plot shows the difference between previous two logs, i.e. the difference between the true formation temperature and the corrected data. The fourth plot shows the radial heat flow q_h.

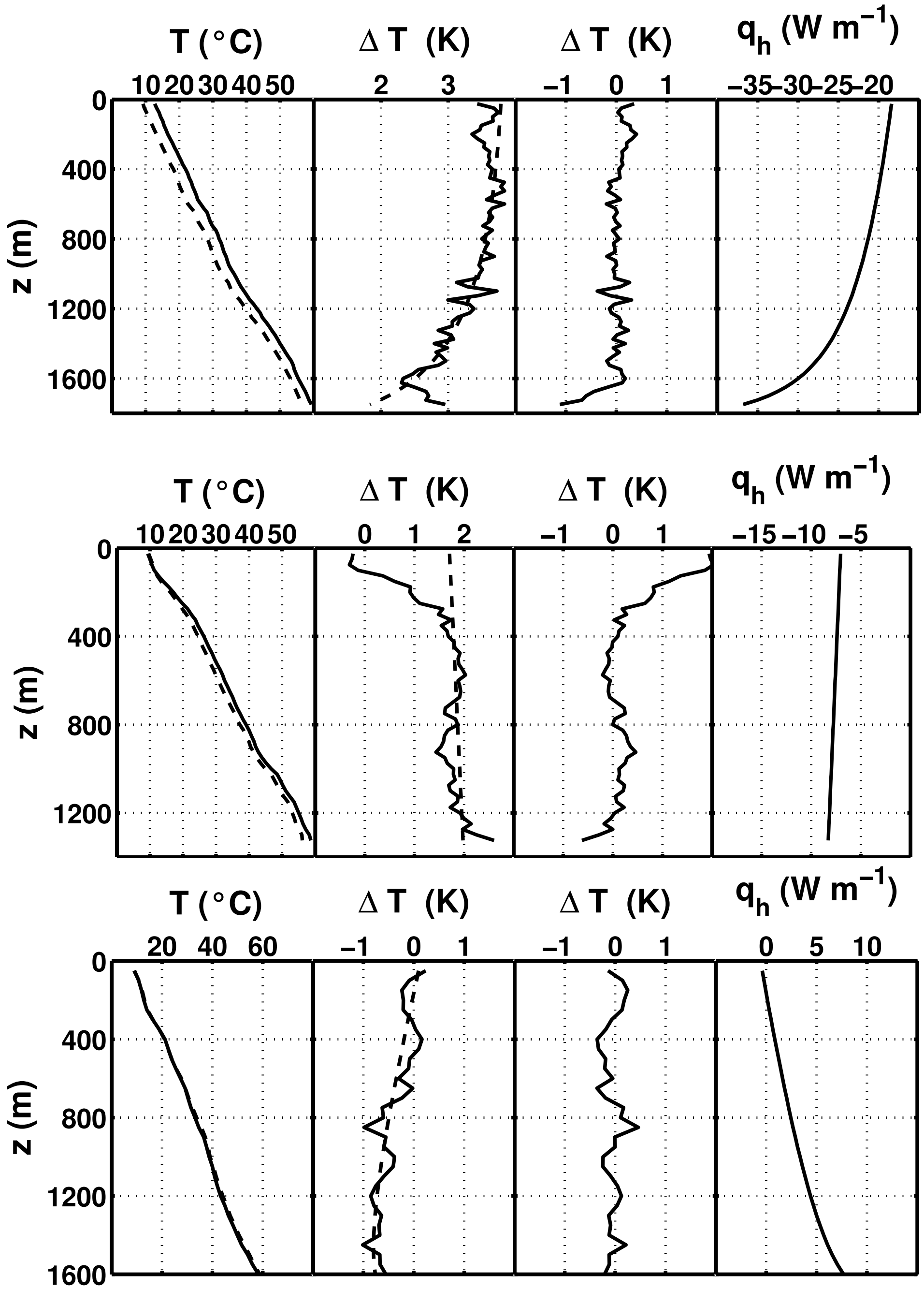

Fig. 4.6: Correction of three measured temperature logs. Explanation of plots from left to right: First plot, dashed curves are the disturbed temperature logs depicted together with the equilibrium formation temperature (solid curve). Dashed curves on the second plot show the calculated correction function which has to be added to the disturbed temperature for a correction. Solid curves are the true correction functions. The third plot shows the difference between corrected temperature logs and equilibrium temperature. The fourth plot shows the radial heat flow.

4.4 Implications of non-equilibrium temperatures for geothermal analysis

The estimation of Darcy flow and the reconstruction of ground surface temperature (GST) history from temperature logs are two important fields of application in geothermal research. This section shows: (1) how the results of both methods are affected by the transient thermal signature of drilling and circulation mud, (2) to what extent these misinterpretations may be improved by the correction, (3) what would be the result if such a transient signal remained unidentified and was interpreted with respect to (a) groundwater flow and (b) GST history.

4.4.1 Groundwater flow

The Péclet number analysis was applied to the synthetic logs of model (a) (Tab. 4.1) to demonstrate the theoretical result if the technically induced signature would be misinterpreted as being the result of vertical groundwater flow.

Tab. 4.2: Results of the Péclet number analysis on synthetic temperature logs of model (a) in Tab. (4.1), either perturbed (pert.) or corrected (corr.). The transient thermal signature of drilling and circulating mud is here interpreted as due to groundwater flow to demonstrate the resulting uncertainty when dealing with perturbed data.

shut-in time (d)		Pe/L (m^{-1})	Pe (1)	v ($m\,s^{-1}$)	v ($mm\,a^{-1}$)
40	pert.	-4.11 E-4	-0.41	-2.95 E-10	9.3
45	pert.	-3.04 E-4	-0.30	-2.18 E-10	6.9
45	corr.	-3.79 E-5	-0.04	-2.72 E-11	0.9
60	pert.	-1.82 E-4	-0.18	-1.30 E-10	4.1
70	pert.	-1.42 E-4	-0.14	-1.02 E-10	3.2
90	pert.	-9.68 E-5	-0.10	-6.94 E-11	2.2

Although the model implies no flow in the host rock, the analyses yield Darcy flow on the order of several $mm\,a^{-1}$ even after a long shut-in time of 2 months (Tab. 4.2). Clearly, the correction of the perturbed log did not fully eliminate the disturbing signature. However, the corrected log shows a significantly better result. The remaining artificial signature corresponds to a signature that would be induced by a downward directed Darcy flow of around 1 $\mathrm{mm\,a^{-1}}$. This is on the order of the resolution of vertical flow in Péclet number analysis. Thus, data sets cleared from drilling transients will be useful for fluid flow analysis within the resolution of the flow analysis, provided they are carefully corrected and interpreted.

4.4.2 Ground surface temperature history

The ground surface temperature (GST) "history" for the synthetic temperature logs is a constant temperature of 10 $^\circ\mathrm{C}$. But inversion algorithms would misinterpret the thermal signature from drilling and circulating mud as due to variations in the surface temperature. To demonstrate this effect, a GST history was inverted from logs of model (a) in Tab. (4.1) using using the approach of Clauser and Mareschal (1995) which assumes pure downward diffusion of the climatic thermal signature, using the software of Hartmann and Rath (2005). Fig. 4.7 shows the results. The temperature logs have shut-in times of 10, 15, 30, 60 days, respectively. The corrected temperature log (curve E in Fig. 4.7) yields the best result. The GST history from Haenel et al. (1988) shows variations which still are one order of magnitude larger.

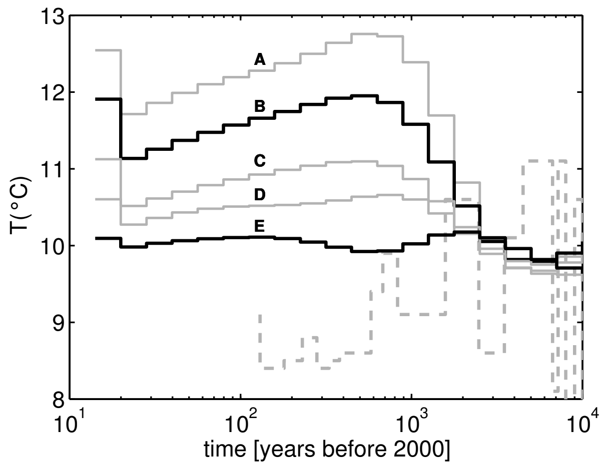

Fig. 4.7: Results of GST inversions of corrected, technically perturbed logs of model (a) (Tab. 4.1) with shut-in time of 10 days (A), 15 days (B), 30 days (C), 60 days (D), respectively. Curve (E) is the inversion result of log (B) after correction of the equilibration transients. The dashed curve is the GST history in central Europe from Haenel et al. (1988).

Fig. (4.7) demonstrates that in the presence of unidentified borehole equilibration transients paleoclimatic inversion of temperature logs will yield completely wrong and useless GST histories. While the correction proposed here does reduce this error, the logs still cannot be used for climatic inversions. These clearly require equilibrated temperature logs. Results from corrected data might provide additional information to the analysis of equilibrated logs if it can be assumed that the correction of the disturbed log was accurate and the log's critical bottom section has been excluded. However, even under optimum conditions, these data sets should be analyzed with extreme caution.

Chapter 5

Discussion

Two novel approaches are presented in this work: One for estimating strata-bound Darcy flow along reservoirs (Chapter 3) and another for improving the quality of technically perturbed temperature logs (Chapter 4). The accuracy and reliability of the results from both methods depend much on the geothermal regime, on data distribution and on availability and quality of temperature data and rock properties. In this chapter, the requirements for application and possible sources of error are discussed.

The method for **estimating strata-bound Darcy flow** was applied on data sets of two sites characterized by very different conditions with respect to spatial data distribution and thermal and hydraulic processes. Both examples do not fully satisfy the requirements of the method, but even under these restrictions a successful analysis is still possible which yields useful information. Several sources of error, however, need to be accounted for.

First of all, the error magnitude depends on the magnitude of the specific discharge rate and the angle subtended by the flow vector and temperature gradient. The term $\vec{v} \cdot \nabla T$ in Eq. (2.11) may become rather small, even in the presence of significant fluid flow, if the angle between temperature gradient and flow approaches 90°. In such a case errors may be large because the flow related thermal signatures becomes small.

An important source of error is associated with the heat flow offset Δq (Eq. 3.5). It is mainly due to the local thermal conductivity and its spatial variability. Estimates of thermal conductivity can be obtained from in-situ experiments, laboratory measurements on core material or inferred from other sources of information. Often, geophysical logs are available at least at some interesting depth intervals, thus allowing the reconstruction of thermal properties with sufficient accuracy and reliability.

A serious potential source of uncertainty arises from the way the local or regional temperature gradient is determined. The example from northern Germany (Chapter 3.3) lacks temperature measurements in the horizon of interest, which is an obvious disadvantage for obtaining reasonable estimates of the temperature gradients in the flow domain. Without further information on the flow regime it is difficult to quantify the error magnitude. But, as the different estimates along the flow path are consistent, the approach seems to be appropriate in this case. However, the example demonstrates that flow can be detected a certain distance from the location of measurement. Generally, under-estimating the gradient leads to over-estimated flow rates.

Constructing smooth surfaces from sparse and scattered data is an ill-posed problem in itself and requires regularization (Billings et al., 2002 a, b). Usually this is achieved by imposing suitable constraints, such as smoothness or related concepts. The derivatives of these surfaces strongly depend on the chosen approximating functions and explicit constraints. Problems arise in case of inappropriate constraints, for instance when smoothness is imposed on a field with biased sampling such as from boreholes near faults. In contrast, local interpolation may be sensitive to data outliers or small-scale disturbances.

A more or less homogeneous flow field is presumed for estimating the flow direction from different projections of the flow vector onto the temperature gradient. In view of data quality it may often be more appropriate to settle for the less informative minimum amplitude estimate based on local linear interpolation, instead of using the more sophisticated but more involved methods to obtain more information. It is advisable to test the results obtained from temperature data by comparing them to additional independent estimates of flow.

An ideal flow estimation requires in particular: (1) high-quality, densely sampled and technically undisturbed temperature logs; (2) laterally and vertically resolved information on thermal conductivity in order to construct vertical heat flow logs from the vertical temperature gradient; (3) a reasonable estimate of the regional temperature gradient; (4) either a reasonably homogeneous flow field or a known flow direction. If any of the requirements is violated, uncertainty will increase. Experience shows, however, that even then important and significant conclusions can be drawn.

Comparison with disturbed and undisturbed temperature logs from identical boreholes showed that the **correction of non-equilibrated temperature logs** can yield a good reconstruction of the undisturbed formation temperature. Small variations of the temperature distribution remain unresolved within a margin of 0.5 K. This may be due to unknown variations in thermal conductivity. A precise determination of the thermal conductivity distribution likely helps to reduce this effect.

Variations in rock thermal conductivity decrease the accuracy of the results. However, the errors are tolerable if the variation in thermal conductivity is moderate, i.e. remains below 25 %. The largest mismatch between the corrected and the equilibrated temperature log is observed in the lower borehole section. In certain cases it might be advisable to remove this part.

The drilling history contains sources of uncertainty that are difficult to quantify. A constant penetration rate during the drilling process is assumed. Also, unknown lateral influx of formation water into the borehole will distort the temperature further. For each individual borehole, the uncertainties of the parameters have to be assessed, in particular those of the drilling history [1]. As the case may be, the errors of the drilling history may be too large or simply unknown and an attempt to correct these data would not necessarily improve the quality.

The infinite line source theory assumes heat to diffuse perpendicular into the matrix. But at the bottom of the borehole one-dimensional heat flow cannot be assumed anymore. Therefore the model is less accurate here.

Obtaining precise temperature data from the ground surface and from BHT reconstruction is difficult. Both may be needed for a correction procedure if non-equilibrated logs are available from nearby. Errors in these input parameters lead to a biased average gradient in the corrected temperature log. The deeper the log the more important this source of error becomes.

[1] Haberland, J. (E.ON Ruhrgas AG), personal communication, 2006

The signature of technical perturbation is of curved shape as is the correction function subtracted from the perturbed log. If an analysis of processes is intended that induce similar thermal signatures, for instance fluid flow, errors in the drilling history will yield biased flow estimations. In the future, the influences of borehole diameter and the behavior of the correction technique for short shut-in times of one or two days need to be studied in more detail.

Chapter 6

Conclusion

This thesis described substantial progress in both issues: flow analysis and correction of perturbed temperature logs. Also, the new findings have practical use for scientists and engineers concerned with the description of flow processes in the deep subsurface. The proposed correction technique for temperature logs has the potential of enlarging considerably the available data base beyond the application to flow analysis. Most existing techniques provided only the vertical component of flow. The examples, however, demonstrate that under favorable conditions magnitude and direction of regional, strata-bound flow in reservoirs can indeed be determined from densely sampled temperature logs.

Although the physics of advective heat transport limits our approach to the thermally effective component of fluid flow, i. e. the one perpendicular to the isotherms, the thermal signature induced by sub-horizontal flow is often sufficiently strong for calculating the specific discharge rate. If the flow direction is known from independent data, the resulting Darcy flow from this approach is most reliable.

In spite of the simplifying assumptions invoked, the analysis provides estimates of small flow rates and their directions as well as estimates of their uncertainty. The results provide a better understanding of the subsurface flow regime and can also be used to constrain a more detailed further analysis such as, e.g., three-dimensional forward and inverse numerical calculations.

The results of the correction demonstrate that the discussed technique is appropriate and sufficient for many geothermal studies based on temperature logs. The mismatch between the corrected temperature log and the equilibrated temperature log is smaller than 0.25 K and 0.5 K for the synthetic example and for the field example, respectively.

This method enables to correct many existing data that up to now could not be corrected. This is because Horner's correction requires a time series of temperature measurements during equilibration. In contrast, the correction technique presented here enables to correct entire temperature logs which were only recorded once. Therefore, the potential data base is much larger than before. The correction function is defined by the drilling history, thermal parameters, and at least two samples of the equilibrium temperature at different depths.

Whether a given corrected temperature log is suitable for a specific analysis depends on its intended use. Note that not only the magnitude of the distortion compared to the desired signal is important. Also its shape may be significant. As shown above (Chapter 4.4), the results of flow estimation may be improved by using corrected logs. In the case of vertical Péclet number analysis the magnitude of the residual bias is near the resolution limit of the method.

The concept of a strata-bound flow analysis (Chapter 3) relies on detailed analysis of anomalies of the vertical heat flow component. They correspond to clear offsets in the heat flow log whereas the error remaining after a correction of transients distorts the calculated vertical heat flow smoothly. Therefore, abrupt changes in vertical heat flow are little affected by residual borehole transients. Their magnitude is much larger than the magnitude of the error. Often, strata-bound flow analysis suffers from a lack of data. Hence, this method will profit considerably from additional data corrected by the proposed technique.

In contrast, the remaining uncertainty is too large for the inversion of ground surface temperature histories (Chapter 4.4.2). Even under optimum conditions, the remaining artefacts will lead to substantial errors. The field examples show that temperature variations of less than 1 K cannot be resolved (Chapter 4.3). Depending on the desired time scale, this generally will not suffice because of the small signal amplitude of paleotemperature effects.

Bibliography

Beardsmore, G. R. and Cull, J. P., *Crustal Heat Flow*, Cambridge University Press, Cambridge, 2001.

Beck, A. E., Shen, P. Y., Beltrami, H., Mareschal, J.-C., Šafanda, J., Sebagenzi, M. N., Vasseur, G., and Wang, K., A comparison of five different analyses in the interpretation of five borehole temperature data sets, palaeogeogr. palaeoclimatol. palaeoecol., *Global Planet. Change Sect.*, *98*, 101–2, 1992.

Bertleff, B., Joachim, H., Koziorowski, G., Leiber, J., Ohmert, W., Prestel, R., Stober, I., Strayle, G., Villinger, E., and Werner, J., *Ergebnisse der Hydrogeothermiebohrungen*, vol. 30, Jb. Geol. Landesamt Baden-Württemberg, Freiburg, 1988.

Billings, S. D., Beatson, R. K., and Newsam, G. N., Interpolation of geophysical data by continuous global surfaces, *Geophysics*, *67*, 1810–22, 2002a.

Billings, S. D., Newsam, G. N., and Beatson, R. K., Smooth fitting of geophysical data using continuous global surfaces, *Geophysics*, *67*, 1823–34, 2002b.

Brandt, S., *Data Analysis*, Springer, Heidelberg-Berlin, 1999.

Bredehoeft, J. H. and Papadopulos, I. S., Rates of vertical groundwater movement estimated from the Earth's thermal profile, *Water Resour. Res.*, *1*, 325–28, 1965.

Bullard, E. C., The time necessary for a borehole to attain temperature equilibrium, *Mon. Not. R. Astron. Soc., Geopys. Supp.*, *5*, 127–30, 1947.

Carslaw, H. S. and Jaeger, J. C., *Conduction of Heat in Solids*, Oxford University Press, London, 1959.

Clauser, C., Opacity – The concept of radiative thermal conductivity, in *Handbook of Terrestrial Heat Flow Density Determination*, edited by R. Hänel, L. Rybach, and L. Stegena, pp. 143–165, Kluwer, Dordrecht, 1988.

Clauser, C., *Untersuchungen zur Trennung der konduktiven und konvektiven Anteile im Wärmetransport in einem Sedimentbecken am Beispiel des Oberrheintalgrabens. In: [anonym.] (Eds), Diss., TU Berlin, Fortschritt-Berichte VDI*, vol. 19(28), VDI Verlag, Düsseldorf, 1988.

Clauser, C., *Thermal Signatures of Heat Transfer processes in the Earth's Crust, Lecture Notes in Earth Sciences*, vol. 85, Springer Verlag, Heidelberg-Berlin, 1999.

Clauser, C., *Geothermal Energy, In: K. Heinloth (Ed), Landolt-Börnstein, Group VIII "Advanced Materials and Technologies", Vol. 3 "Energy Technologies", Subvol. C "Renewable Energies*", Springer Verlag, Heidelberg-Berlin, 2nd. edn., 2006.

Clauser, C. and Mareschal, J.-C., Ground temperature history in central Europe from borehole temperature data, *Geophys. J. Int.*, *121(3)*, 805–817, 1995.

Clauser, C. and Villinger, H., Analysis of conductive and convective heat transfer in a sedimentary basin, demonstrated for the Rheingraben, *Geophys. J. Int.*, *100*, 393–414, 1990.

Clauser, C., Giese, P., Huenges, E., Kohl, T., Lehmann, H., Rybach, L., and Šafanda, J., The thermal regime of the crystalline continental crust: Implications from the KTB, *J. Geophys. Res*, *102*, 18 417–41, 1997.

Clauser, C., Deetjen, H., Hartmann, A., Höhne, F., Rath, V., Rühaak, W., Schellschmidt, R., Wagner, R., Wolf, A., and Zschocke, A., *Erkennen und Quantifizieren von Strömung: Eine geothermische Rasteranalyse zur Klassifizierung des tiefen Untergrundes in Deutschland hinsichtlich seiner Eignung zur Endlagerung radioaktiver Stoffe - Fortsetzung (9WS 0009 - 8497-2). Endbericht der Geophysica Beratungsgesellschaft mbH (10. November 2004), Tech. Rep.*, Angewandte Geophysik RWTH Aachen, Hochleistungsrechnen RWTH Aachen and GGA-Institut, Aachen, 2004.

Darcy, H., *Les fontaines publiques de la ville de Dijon*, Springer Verlag, Dalmont, Paris, 1856.

Dowdle, W. L. and Cobb, W. M., Static formation temperature form well logs, an empirical method, *Journal of Petroleum Technology*, *27*, 1326–30, 1975.

Edwardson, M. J., Girner, H. M., Parkison, H. R., Williams, C. D., and Matthews, C. S., Calculation of formation temperature disturbances caused by mud circulation, *J. Petrol. Technol.*, *14*, 416–26, 1962.

Grissemann, C. and Czora, C., Geothermische Untersuchungen in den hydrogeologischen Bohrungen des Erkundungsgebietes Dömitz-Lenzen, Abschlussbericht 9G3411600000 im Auftrag des Bundesamtes für Strahlenschutz, Tech. rep., Bundesanstalt für Geowissenschaften, 2003.

Haenel, R., Rybach, L., and Stegena, L. (eds.), *Handbook of terrestrial heat-flow density Determination (Guidelines and reccommendations of the International Heat-Flow Comission)*, Solid Earth Science, Kluwer Academic Publishers, Dordrecht (D. Reidel Publ. Comp.), 1988.

Hartmann, A. and Rath, V., Uncertainties and shortcomings of ground surface temperature histories derived from inversion of temperature logs, *Journal of Geophysics and Engineering*, *2*, 299–311, 2005.

Hartmann, A., Rath, V., and Clauser, C., Thermal conductivity from core and well log data, *Int. J. Rock Mechanics and Mining Sciences*, *42*, 1042–55, 2005.

Horner, D., *Pressure Build-up in Wells - Proc.*, vol. 34, Third World Petroleum Congress, Section 2, The Hague, 1951.

Jaeger, J. C., The effect of the drilling fluid on temperatures measured in boreholes, *J. Geophys. Res.*, *66(2)*, 563–69, 1961.

Kessels, W., Abschätzung der zu erwartenden Temperaturstörungen im Gebirge durch das Erstellen der Kontinentalen Tiefbohrung der Bundesrepublik Deutschland (KTB), in *KTB-Report 88-4*, pp. 155–77, Draxler, J. K., Hänel, R., Niedersächsisches Landesamt für Bodenforschung, Hannover, 1988.

Klinge, H., Schelkes, K., Rübel, A., Suckow, A., Schildknecht, F., and Ludwig, R., The saltwater/freshwater regime in the sedimenatary cover of the Gorleben salt dome, *Transport in Porous Media*, *47*, 125–48, 2002.

Kohl., T., Signorelli, S., and Rybach, L., Three-dimensional (3-d) thermal investigation below high alpine topography, *Physics of the Earth and Planetary Interiors*, *126*, 195–210, 2001.

Kronmüller, K., *Sedimentologie der Bausteinschichten und der Unteren Cyrenenschichten im westlichen Molassebecken Süddeutschlands (Oberoligozän)*, Doctoral Dissertation, Tech. Univ. Clausthal, 1987 a.

Kronmüller, R., *Diagenese der kalzitisch zementierten karbonatreichen Sandsteine der Bausteinschichten (Oberoligozän, Süddeutsche Westmolasse)*, Doctoral Dissertation, Tech. Univ. Clausthal, 1987 b.

Kutasov, I., *Applied Geothermics For Petroleum Engineers*, Elsevier, Santa Monica, CA 90401, USA, 1999.

Lachenbruch, A. H. and Brewer, M. C., *Dissipation of the temperature effect of drilling a well in arctic Alaska.*, vol. 1083C, Anchorage, AK, USA, 1959.

Mansure, A. J. and Reiter, M., A vertical groundwater movement correction for heat flow, *J. Geophys. Res.*, *84*, 3490–96, 1979.

Mareschal, J.-C. and Beltrami, H., Evidence for recent warming from perturbed geothermal gradients: Examples from eastern Canada, *Clim. Dyn.*, *6*, 135–43, 1992.

Paschen, H., Oertel, D., and Grünwald, R., Möglichkeiten geothermischer stromerzeugung in deutschland, sachstandsbericht, Tech. rep., Büro für Technikfolgenabschätzung (TAB) des Deutschen Bundestages, 2003.

Pollack, H. N., Hurther, S. J., and Johnson, J. R., Heat flow from the Earth's inerior: Analysis of the global data set, *Reviews of Geophysics*, *31(3)*, 267–80, 1993.

Popov, Y. A., Sass, J. H., Williams, C. F., and Burkhardt, H., Characterization of rock thermal conductivity by high-resolution optical scanning, *Geothermics*, *28*, 253–76, 1999.

Pribnow, D. and Schellschmidt, R., Thermal tracking of upper crustal fluid flow in the Rhine Graben, *Geophys. Res. Lett.*, *27*, 1957–60, 2000.

Ramey, H. J., Wellbore heat transmission, *J. Petrol. Technol.*, *14*, 427–35, 1962.

Raymond, L. R., Temperature distribution in a circulating drilling fluid, *J. Petrol. Technol.*, *21*, 333–41, 1969.

Reiter, M., Using precision temperature logs to estimate horizontal and vertical groundwater flow components, *Water Resources Research*, *37*, 663–74, 2001.

Sass, J. H. and Lachenbruch, A. H., *Preliminary interpretation of thermal data from the Nevada test side*, vol. 82-973 of *Open-File Report*, U. S. Geol. Survey, Menlo Park, CA, USA, 1982.

Schellschmidt, R. and Zschocke, A., Karten des Temperaturfeldes im Untergrund Deutschlands, *online in internet: WWW: http://www.gga-hannover.de/institut/verschiedenes/daten/tem_daten/home.htm*, 2003.

Schildknecht, F., *Dichteschichtung und Druckverteilung im salinen Grundwasser des Untersuchungsgebietes Dömitz-Lenzen Endbericht AP9G3411200000 im Auftrag des Bundesamtes für Strahlenschutz*, Bundesanstalt für Geowissenschaften und Rohstoffe, Tech. Rep., Hannover, 1999.

Shen, P. and Beck, A. E., Paleoclimate change and heat flow density inferred from temperature data in the superior province of the Canadian shield, *Palaeogeogr. Palaeoclimatol. Palaeoecol. (Global Planet. Change Sect.)*, *98 (B12)*, 143–65, 1992.

Shen, P. Y. and Beck, A. E., Least square inversion of borehole temperature measurements in functional space, *Journal of Geophysical Research*, *96 (B12)*, 19 965–97, 1991.

Stallman, R. W., *Computation of Ground-Water Velocity from Temperature Data*, vol. 1544-H, U.S. Geolog. Survey Water-Supply Paper, Washington, DC., USA, 1963.

Taniguchi, M., Shimada, J., Tanaka, T., Kayane, I., Sakura, Y., Shimano, Y., Dapaah-Siakwan, S., and Kawashima, S., Disturbance of temperature-depth profiles due to surface climate change and subsurface water flow, 1. an effect of linear increase in surface temperature by global warming and urbanization in the (Tokyo) metropolitan area, (Japan), *Water Resources Research*, *35(5)*, 1507–17, 1999a.

Taniguchi, M., Williamson, D. R., and Peck, A. J., Disturbance of temperature-depth profiles due to surface climate change and subsurface water flow, 2. an effect of step increase in surface temperature caused by forest clearing in southwest western Australia, *Water Resources Research*, *35(5)*, 1519–29, 1999b.

Tarantola, A. and Valette, B., Generalized nonlinear inverse problems solved using the least square criterion, *Rev. Geophys. Space Phys.*, *20*, 219–32, 1982.

Theis, C., The relation between the lowering of the piezometric surface and the rate and duration of discharge of a well using groundwater storage, *Trans. Amer. Geophys. Union*, *16*, 519–24, 1935.

van der Kamp, G. and Bachu, S., Use of dimensional analysis in the study of thermal effects of various hydrogeological regimes, in *Hydrogeological regimes and their subsurface thermal effects*, edited by A. E. Beck, G. Garven, and L. Stegena, vol. 47 of *Geophysical Monograph*, pp. 23–28, Am. Geophys. Union, Washington, 1989.

van Schmus, W. R., *in: Ahrens, T.J. (Ed), Global Earth Physics a Handbook of Physical Constants, AGU Reference Shelf 1*, vol. 283–91, Am. Geophys. Union, 1995.

Vasseur, G. and Demongodin, L., Convective heat transfer in sedimentary basins, *Basin Res.*, *7*, 67–79, 1995.

Vasseur, G., Lucazeau, F., and Bayer, R., The problem of heat flow density determination from inaccurate data, *Tectonophysics*, *121*, 25–34, 1985.

Ziagos, J. P. and Blackwell, D. D., A model for the effect of horizontal fluid flow in a thin aquifer on temperature-depth profiles, *Geotherm. Resour. Counc. Trans.*, *5*, 221–23, 1981.

Appendix

A.1 Logs of vertical heat flow in the Gorleben area

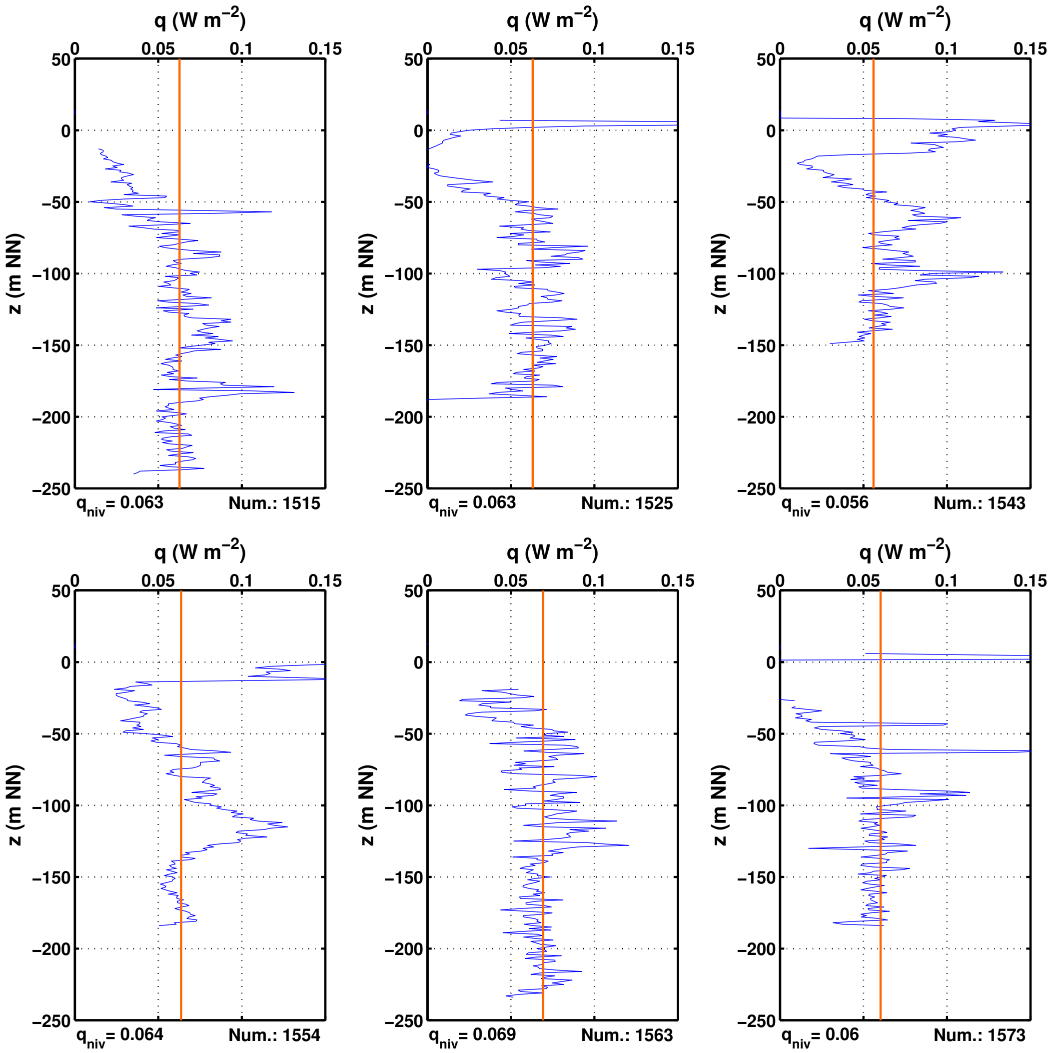

See below for figure caption.

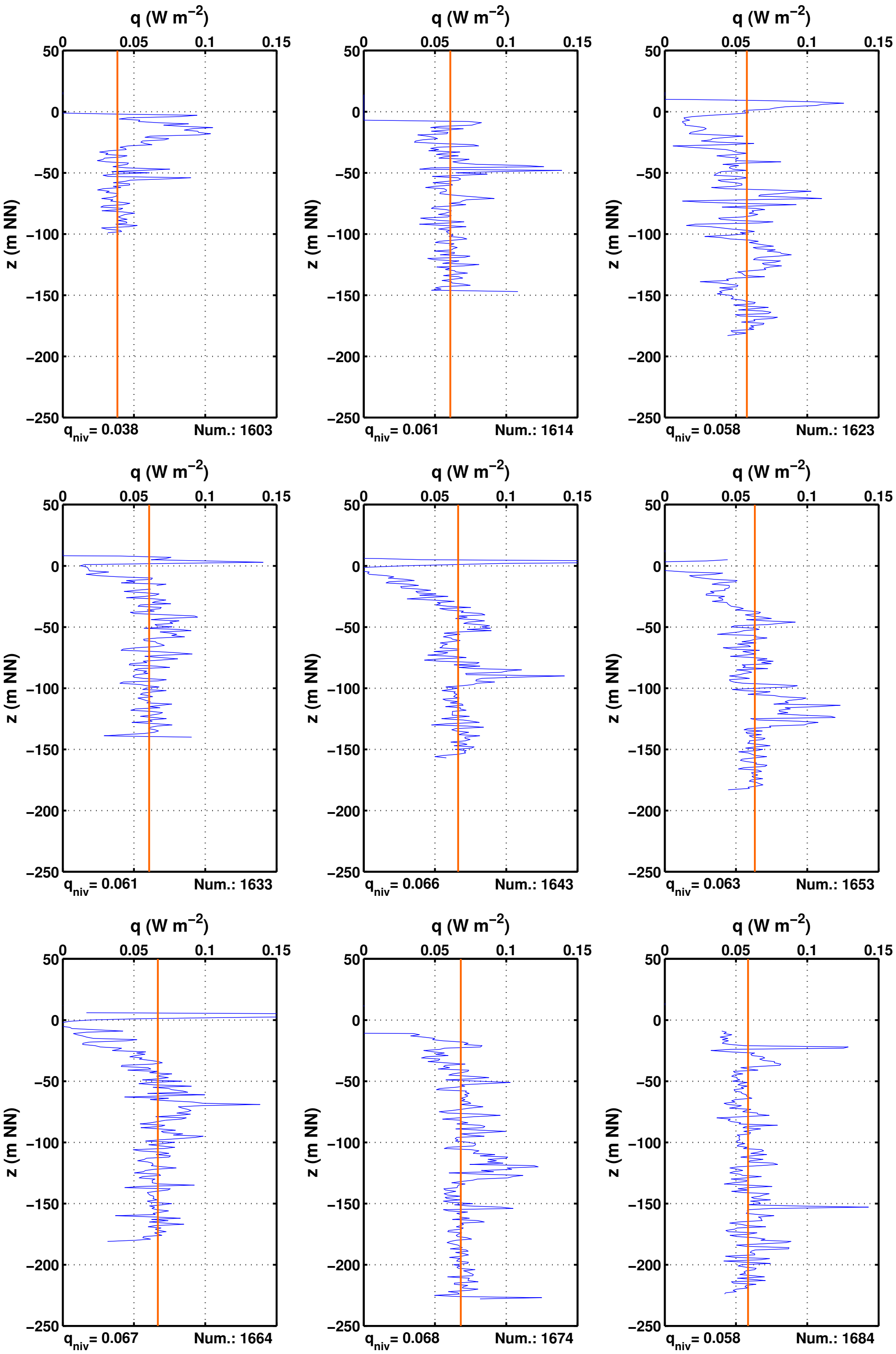

See below for figure caption.

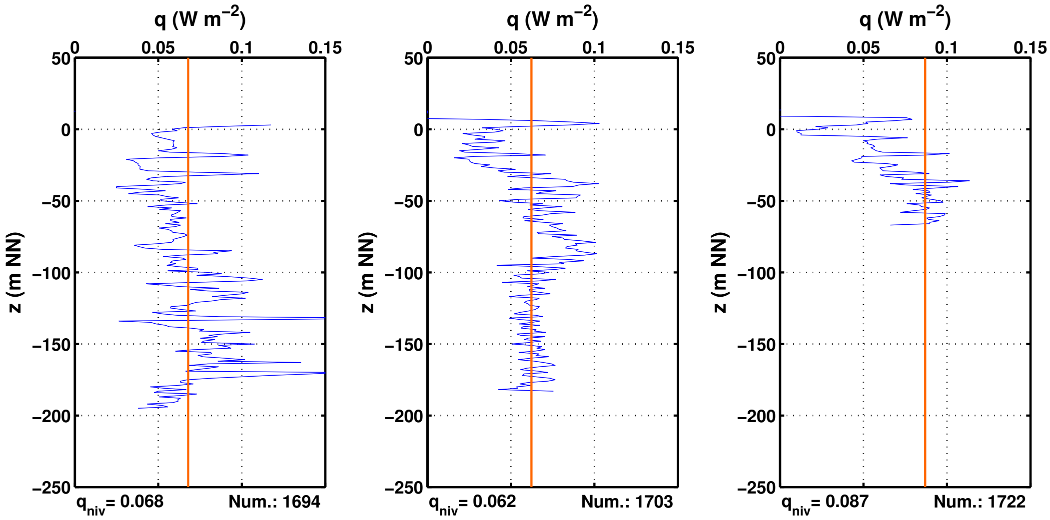

Fig. A.1: Logs of vertical specific heat flow in the Gorleben area calculated according to Fourier's law (Eq. 2.3). Depth is referenced to sea level (a.s.l.).

Curriculum Vitae

Personal Data	Born on the 23th of March 1975 in Berlin, German
Employments	since *11/15/2005* Geoscientist at E.ON-Ruhrgas AG Reservoirs and Storage Facilities Competence Centre
	07/01/2005 - 09/30/2005 Co-author of the study "Potential of the Malm karst aquifer for geothermal energy recovery", Leibniz Institute for Applied Geosciences
	11/01/2004 - 02/28/2005 Co-author of the "Feasibility study on the production of a geothermal atlas for Germany", Leibniz Institute for Applied Geosciences
	10/16/2000 - 10/31/2004 Scientist at the Leibniz Institute for Applied Geosciences, Groundwater and Geothermics Section, project: "Geothermische Rasteranalyse"
	06/01/1996 - 10/14/1997 Tutor at the Technical University of Berlin, Institute for Applied Geosciences
Studies	*10/1994 - 04/1999* Applied Geosciences at the Technical University of Berlin (TU-Berlin), Hydrogeology
	Diploma Thesis: "Hydrochemistry of the groundwater in Caldas Novas -Central Brasil-, implications for the thermal reservoir"
	Degree: Diplom-Ingenieur, Hydrogeologist, passed with distinction
Awards	Award for young authors of the *Deutsche Geophysikalische Gesellschaft* at the 62th annual meeting in Jena, Germany, 24.02.2003, for the oral presentation at the annual meeting in 2002, Hannover, Germany.

Curriculum Vitae

Zur Person	geboren am 23.03.1975 in Berlin, deutsch
Tätigkeiten	*seit Nov. 2005* Geowissenschaftler bei der E.ON-Ruhrgas AG Kompetenz-Center Speicher und Lagerstätten
	Jul. 2005 - Sep. 2005 Co-Autor der Studie „Hydraulische Eigenschaften des Malmkarstes und Untergrundtemperaturen im Süddeutschen Molassebecken", GGA-Institut
	Nov. 2004 - Feb. 2005 Co-Autor der „Machbarkeitsstudie zur Erstellung eines Geothermischen Atlas für Deutschland", GGA-Institut
	Okt. 2000 - Okt. 2004 Wissenschaftlicher Angestellter am GGA-Institut, Sektion Geothermik und Grundwasserhydraulik, Projekt: „Geothermische Rasteranalyse"
	Jun. 1996 - Okt. 1997 Tutor am Institut für Angewandte Geowissenschaften, TU-Berlin
Studium	*Okt. 1994 - Apr. 2000* Geoingenieurwissenschaften und Angewandte Geowissenschaften, Technische Universität Berlin, Vertiefungsrichtung Hydrogeologie
	Diplomarbeit: „Zur Hydrochemie der Grundwässer von Caldas Novas -Zentralbrasilien-, Implikationen für das Thermalgrundwasser"
	Abschluss: Diplom-Ingenieur, Vertiefung Hydrogeologie, mit Auszeichnung
Auszeichnung	Auszeichnung für Beiträge junger Autoren der Deutschen Geophysikalischen Gesellschaft auf der 62. Jahrestagung in Jena, 24.02.2003, für den Vortrag „Quantifizierung schichtfolgender Grundwasserströmung anhand von korrelierten Sprüngen im vertikalen Wärmestrom" auf der Jahrestagung 2002 in Hannover.